

RF SENSOR ANTENNA FOR FOOD ADULTERATION DETECTION

PROJECT REPORT

*Submitted to
the APJ Abdul Kalam Technological University
in partial fulfillment of the requirement for the award of Degree of
Bachelor of Technology in Electronics and Communication Engineering*



BY
K I AJAY MENON(NSS16EC044)
PRANAV S (MDL16EC086)
SACHIN GOVIND (MDL16EC092)
YADHUKRISHNA MADHU (MDL16EC119)

*Department of Electronics,
Model Engineering College,
Thrissur, Kochi-682021,
Kerala.*

JUNE 2020

**DEPARTMENT OF ELECTRONICS
MODEL ENGINEERING COLLEGE
THRIKKAKARA, KOCHI-682021**



CERTIFICATE

This is to certify that this Project entitled ***RF SENSOR ANTENNA FOR FOOD ADULTERATION DETECTION*** is the bonafide record of work carried out by **K I AJAY MENON (NSS16EC044)**, **PRANAV S (MDL16EC086)**, **SACHIN GOVIND (MDL16EC092)** and **YADHUKRISHNA MADHU (MDL16EC119)** in partial fulfillment of the requirements for the completion of Degree of Bachelor of Technology in Electronics and Communication Engineering, at the Department of Electronics, Model Engineering College, Thrikkakara, Kochi.

Dr. Rajesh Mohan R Arun C R

Dr. Laila D

Project Guide Project co-ordinator Head of the Department

ACKNOWLEDGEMENT

We would like to express our sincere gratitude to everyone who assisted us in conducting this Project. Our heartfelt gratitude to the coordinator Assistant Prof.Arun C R, Department of Electronics, for giving us permission to commence this Project. We express our sincere gratitude to Principal Prof.(Dr.)Vinu Thomas and Prof.(Dr.)Laila D, HOD, Electronics and Communication Engineering, Model Engineering College. Special thanks to Our guide Prof.(Dr.)Rajesh Mohan R, Department of Electronics, whose guidance and encouragement helped us through out this endeavour.

ABSTRACT

In this project, a non-destructive technique is presented for detection of adulteration in common food items using the proposed microwave planar resonant sensor. The proposed sensor is operating in the ISM (industrial, scientific and medical) frequency band of 5.7 GHz. The sensor is designed using the ANSYS HFSS, the CST Microwave Studio and an empirical model of the proposed sensor is developed for the accurate calculation of complex permittivity of standard food samples under test in terms of the resonant frequency. The developed model is then used to detect the percentage adulteration of contaminants in the pure food samples. The designed resonant sensor is fabricated on a 1.6 mm FR4 substrate. A sample container made of borosilicate glass is specially designed to make the overall procedure to be non-contacting and non-destructive. The fabricated sensor is finally tested for detecting adulteration with different concentration levels in food samples. Using change in resonance frequency, with the help of algorithm percentage of adulterants can be predicted in real time.

Contents

1	Introduction	1
1.1	Microwave	2
1.2	Microstrip Sensor Antenna	3
1.3	Microwave Characteristics of Food-items	5
1.4	Motivation	7
1.5	Problem Statement and Objectives	7
1.6	Thesis Outline	8
2	State Of Art	11
2.1	Food Adulteration and Evaluation	11
2.2	Examples of Adulterated Foods	12
2.3	Analytical Methods for the Detection of Adulteration	14
2.3.1	Analysis of the Headspace Gaseous Phase of Products .	14
2.3.2	Solid-phase Microextraction	15
2.3.3	Mass Spectrometry	17
2.3.4	Electronic Nose and Electronic Tongue	18
2.3.5	Fourier Transform Infrared Spectroscopy	21
2.3.6	Nuclear Magnetic Resonance Spectroscopy	23
2.3.7	Raman Spectroscopy	25
2.3.8	Infrared Spectroscopy	27
2.3.9	High-Performance Liquid Chromatography	29

2.3.10 Hyperspectral Imaging	32
2.4 Detection of Food Adulteration using Microwave Antenna over Conventional Methods	34
3 Working	36
3.1 Theory	36
3.2 Principle	37
3.3 Structure and Design	39
3.4 Simulation	41
3.4.1 CASE 1	42
3.4.2 CASE 2	43
3.4.3 CASE 3	44
3.4.4 CASE 4	44
3.4.5 CASE 5: VOLUMETRIC ANALYSIS	46
3.5 MODELLING	47
4 Fabrication and Testing	50
4.1 Fabrication of Sensor antenna	50
4.1.1 Photolithography	51
4.2 Experimental Setup	53
4.2.1 VNA Master 2026C	54
4.3 Antenna Testing	55
5 Conclusion	58
Bibliography	59

List of Figures

1.1	Electromagnetic Spectrum	3
1.2	Microwave Frequency Bands	4
1.3	Microwave Sensor	5
1.4	Phases of project	9
1.5	Proposed Model	10
2.1	Headspace Gas Chromatography	15
2.2	Solid-phase Microextraction	16
2.3	Quadrupole Mass Spectrometer	18
2.4	Electronic Nose and Electronic Tongue	19
2.5	Electronic Nose and Electronic Tongue Circuit	20
2.6	Fourier Transform Infrared Spectroscopy Setup	21
2.7	Fourier Transform Infrared Spectrometer	23
2.8	Nuclear Magnetic Resonance Spectroscopy	24
2.9	Nuclear Magnetic Resonance Spectrometer	25
2.10	Raman Spectroscopy	26
2.11	Raman Scattering	27
2.12	Infrared Spectroscopy	28
2.13	High-Performance Liquid Chromatography	30
2.14	High-Performance Liquid Chromatography Setup	31
2.15	Hyperspectral Imaging	32

2.16 Hyperspectral Imaging in Foods	34
3.1 Simulation setup in HFSS	38
3.2 Antenna dimensions	39
3.3 Implementation of resonant structures using CSW and slotted lines	40
3.4 Electric field intensity distribution	41
3.5 Simulation setup for MUT below sensor	42
3.6 S21 for MUT below sensor	42
3.7 Simulation setup for MUT at a height 1mm above sensor	43
3.8 S21 for MUT at a height 1mm above sensor	43
3.9 Simulation setup for MUT in contact with the sensor	44
3.10 S21 for MUT in contact with the sensor	44
3.11 S21 of air with relative permittivity=1.008	45
3.12 S21 of material with relative permittivity=5.7	45
3.13 S21 of material with relative permittivity=6.8	46
3.14 S21 of fresh water with relative permittivity=81	46
3.15 Volumetric Analysis	47
3.16 Relative permittivity v/s Resonant frequency	49
3.17 Approximation of the dataset using logarithmic and power functions	49
4.1 Placing structure in x-y plane	51
4.2 Saving the file	52
4.3 Structure printed in transparent sheet	52
4.4 Fabricated antenna	54
4.5 VNA Master 2026C front view	55
4.6 VNA Master 2026C back view	56
4.7 Final structure	57

List of Tables

3.1	Volumetric analysis table	47
3.2	Resonant Frequency Vs Relative Permittivity	48

Chapter 1

Introduction

Food adulteration has a long history in human society, and it still occurs in modern times. Because children are relatively vulnerable to food adulterants, studying the health impacts of food adulteration on children is important. To detect food adulteration and to avoid further harm caused by food adulteration, simple screening methods have been developed and they have recently emerged as a new focus area for research. With regard to food, the term “quality” means the products meet the requirements of an entire complex of criteria, properties and peculiarities, which characterize the product’s degree of suitability based on its assessment and consumption. “Food safety” is a condition that ensures food will not cause harm to the consumer when prepared and consumed according to its intended use. It entails the handling, preparation and storage of food in ways that prevent food borne illness. Quality and safety remains a major challenge in the production of high quality foods[3].

Our project focuses on detecting food adulterants by non-destructive means by using microwave sensor antenna. Microwave sensor interacts with matter to measure properties, and it can be used to sense the moisture content, density, structure and shape of materials, and even chemical reaction. Advantages of microwave sensor over traditional sensor is its speed of measurement, non-destructive, precise, fully automated and it can

be made in a laboratory or online. These have the potential to be ubiquitous and shape the upcoming industrial facilities, medical diagnostic systems and food safety detection.

A major distinction between destructive and non-destructive procedures is that destructive analysis is typically used to identify an adulterant that has been added to or removed from a product and to assess the range in concentration. When possible, non-destructive methods are then developed for specific adulterants or a small group of similar adulterants. Non-destructive analyses tend to be less precise than traditional chemical analyses but have the advantage of speed, lower cost and often allow assessing each product unit rather than a sample of an entire volume. Assessing each product unit is important when the adulterant is not uniform (when adulterated individual fruit are mixed in with non-adulterated fruit) and each product unit must be individually assessed. This is especially critical when consumer health is imperiled by the adulterant. In such cases, a non-destructive means of monitoring each individual product unit is required.

1.1 Microwave

Microwaves are electromagnetic radiation with frequencies between 300 MHz and 300 GHz, corresponding to wavelengths ranging from as long as one meter to as short as one millimeter. International agreements regulate the use of the different parts of the microwave spectrum. The frequencies 915 MHz and 2.45 GHz are the most common among those dedicated to power applications for Industrial, Scientific and Medical purposes. In all cases, microwaves include the entire SHF band (3 to 30 GHz, or 10 to 1 cm) at minimum. Frequencies in the microwave range are often referred to by their IEEE radar band designations: S, C, X, Ku, K, or Ka band. The proposed microwave sensor work under C band.

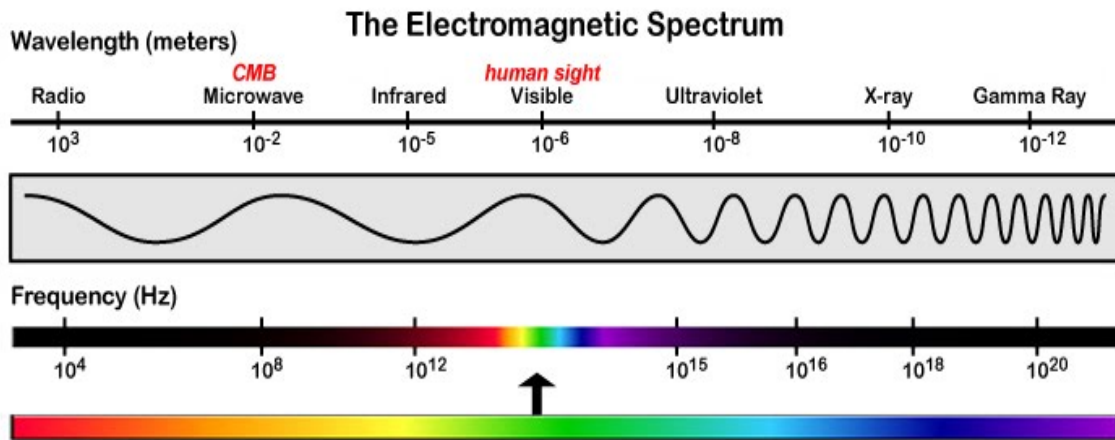


Figure 1.1: Electromagnetic Spectrum

Microwaves travel by line-of-sight; unlike lower frequency radio waves they do not diffract around hills, follow the earth's surface as ground waves or reflect from the ionosphere. So terrestrial microwave communication links are limited by the visual horizon to about 40 miles (64 km).

1.2 Microstrip Sensor Antenna

In telecommunication, a microstrip antenna (also known as a printed antenna) usually means an antenna fabricated using microstrip techniques on a printed circuit board (PCB). It is a kind of internal antenna; they are mostly used at microwave frequencies. An individual microstrip antenna consists of a patch of metal foil of various shapes (a patch antenna) on the surface of a PCB (printed circuit board), with a metal foil ground plane on the other side of the board. Most microstrip antennas consist of multiple patches in a two-dimensional array. The antenna is usually connected to the transmitter or receiver through foil microstrip transmission lines. The radio frequency current is applied (or in receiving antennas the received signal is produced) between the antenna and ground plane. Devices having microwave sensors generate microwave signals which cover certain area across the space. When an object is placed in front of the microwave zone, it causes waves to reflect. This is detected by the sensor to measure

Microwaves Frequency Bands

Band	Frequency range
HF Band	3 to 30 MHz
VHF Band	30 to 300 MHz
UHF Band	300 to 1000 MHz
L Band	1 to 2 GHz
S Band	2 to 4 GHz
C Band	4 to 8 GHz
X Band	8 to 12 GHz
Ku Band	12 to 18 GHz
K Band	18 to 27 GHz
Ka Band	27 to 40 GHz
V Band	40 to 75 GHz
W Band	75 to 110 GHz
mm Band	110 to 300 GHz

Figure 1.2: Microwave Frequency Bands

properties.

There are different RF material characterization techniques available, which can be divided under the non-resonant and resonant methods. The non-resonant methods are normally used for wideband characterization of samples with moderate accurate results and hence the resonant methods are preferred over non-resonant methods for obtaining accurate results over narrow band of operation. Among the RF resonant methods, the liquid characterization can be performed either using the cavity resonators or with

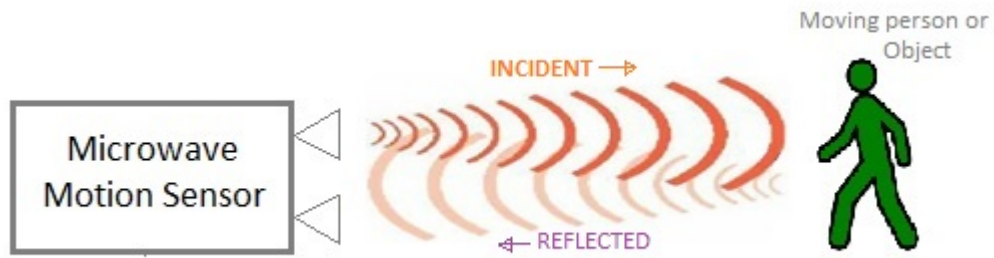


Figure 1.3: Microwave Sensor

the help of planar resonant sensors. Since cavity resonator method requires bulky and costly metallic cavities, the planar resonant sensors are preferred because of advantages such as low cost, easy fabrication, easy integration with other microwave circuits etc. For the implementation of planar resonant methods, various resonant structures such as combination of series resonators (SR), inter-digitated capacitor (IDC), split ring resonator (SRR), complementary split ring resonator (CSRR) have been used. Additionally, the planar sensors are fabricated using both the microstrip and the coplanar waveguide technologies. Among these different resonant structures, the IDC and some specialized resonators are fabricated on the main microstrip line. On the contrary, in the case of the SRR and CSRR structures, the resonant structure is coupled to the microstrip line either electrically or magnetically depending upon the orientation of the resonator with the microstrip line. Since the IDC type resonators are fabricated on the main transmission line using the microstrip technology, they are easy to get fabricated and provide reasonably higher amount of sensitivity[1].

1.3 Microwave Characteristics of Food-items

The internal factors of food products including physical, chemical and microbial features are very important parameters which are strongly influenced by the properties such as composition and storage time. Food of different compositions differs in dielectric properties including permittivity

and conductivity that determine how it reacts to an external electromagnetic field. Since the moisture content and composition of fresh food should be in a reasonable range, the dielectric properties of fresh food should be also in a certain level. Therefore, the spoilage and water evaporation of food can be determined by measuring the change in dielectric properties. In addition, the salt content, ingredients and contamination affecting the dielectric properties of food materials can be measured and evaluated. The microwave sensor systems are designed to evaluate the quality of food by determining the dielectric properties of food through its influence to the propagation of microwave in the forms reflection, penetration, transmission, scattering and resonance[2].

The fundamentals of microwave sensors are based on the fact that the interaction between microwaves and the medium of propagation is determined by the complex relative permittivity and relative permeability of the medium.

$$\epsilon_r = \epsilon' - \epsilon''$$

$$\mu_r = \mu' - \mu''$$

Here ϵ' signifies the ability to store electric energy and ϵ'' , the ability to convert electric energy into heat. Here μ' and μ'' represent respectively the portion of magnetic energy stored and lost in a material. However, since food materials have low influence on magnetic field, the measurements are mainly determined by ϵ' and ϵ'' , which are called dielectric constant and loss factor.

Microwave sensor determines the dielectric properties in propagation of electromagnetic field to reveal the parameters of food objects mainly through three measurement modes, reflection, transmission and resonation. In order to illustrate the transmission of microwave in the measurement, the following model is concentrated on the special case for planar samples in

free-space.

1.4 Motivation

We beings are more concerned about our standard of living and mainly our health. For good health we need good food, but the real question is that "are we getting good food?". Today almost everything we eat today are adulterated from everyday using oils to packed food items from store. There are mainly two factors that ensures good food are "safety" and "quality". As engineers we are obliged to do something good for the society. So we started this project to bring a standardised testing method for detection of food adulteration in real-time.

1.5 Problem Statement and Objectives

In the present world that we are living almost everything we consume are mostly adulterated. To detect food adulteration and to avoid further harm caused by food adulteration, simple screening methods have been developed and they have recently emerged as a new focus area for research. With regard to food, the term "quality" means the products meet the requirements of an entire complex of criteria, properties and peculiarities, which characterize the product's degree of suitability based on its assessment and consumption. "Food safety" is a condition that ensures food will not cause harm to the consumer when prepared or eaten according to its intended use. It entails the handling, preparation, and storage of food in ways that prevent food borne illness. Quality and safety remains a major challenge in the production of high quality foods. To assess quality and safety of food we developed a standard RF based sensor antenna for detection of adulterants in food items and to ensure safety and quality of food items should be maintained.

The objectives are :

1. To learn impact of food in human health.

2. To learn more on high frequency sensors.
3. To learn various tools used for high frequency analysis.
4. To study, implement and test a high frequency food adulteration testing sensor antenna .
5. Propose a model for real-time testing and analysis of adulterants in food items.
6. To ensure food safety and quality.

1.6 Thesis Outline

The proposed model is focused on detecting adulterants in food. The sensor is an IDC (Inter-digitated capacitor) structure which is a resonant planar structure. Sensor is designed using ANSYS HFSS software and is simulated using HFSS and CST Studio. Most of the planar resonant RF sensors are based on the electromagnetic (EM) field perturbation approach. Since the electric field in the resonant structure is mainly responsible for the characterization of MUT (material under test), the MUT is kept in close contact with the resonant structure of the sensor. The electric field confined to the resonant structure of the RF sensor interacts with the MUT at the resonant frequency. The loading of MUT on the sensor changes the effective capacitance of the equivalent circuit of the resonant structure, which causes a shift in resonant frequency. This resonant frequency shift of the sensor is mainly attributed to the real part of the complex permittivity of the MUT. This frequency shift is used to identify percentage of adulterants in food item using algorithm as real-time analysis.

In the proposed sensor design, a folded type open stub and short stub are used as the resonating structures which are designed on the main line of microstrip structure. The structure is designed using the full wave electromagnetic solver, the CST Microwave Studio and the dimensions of

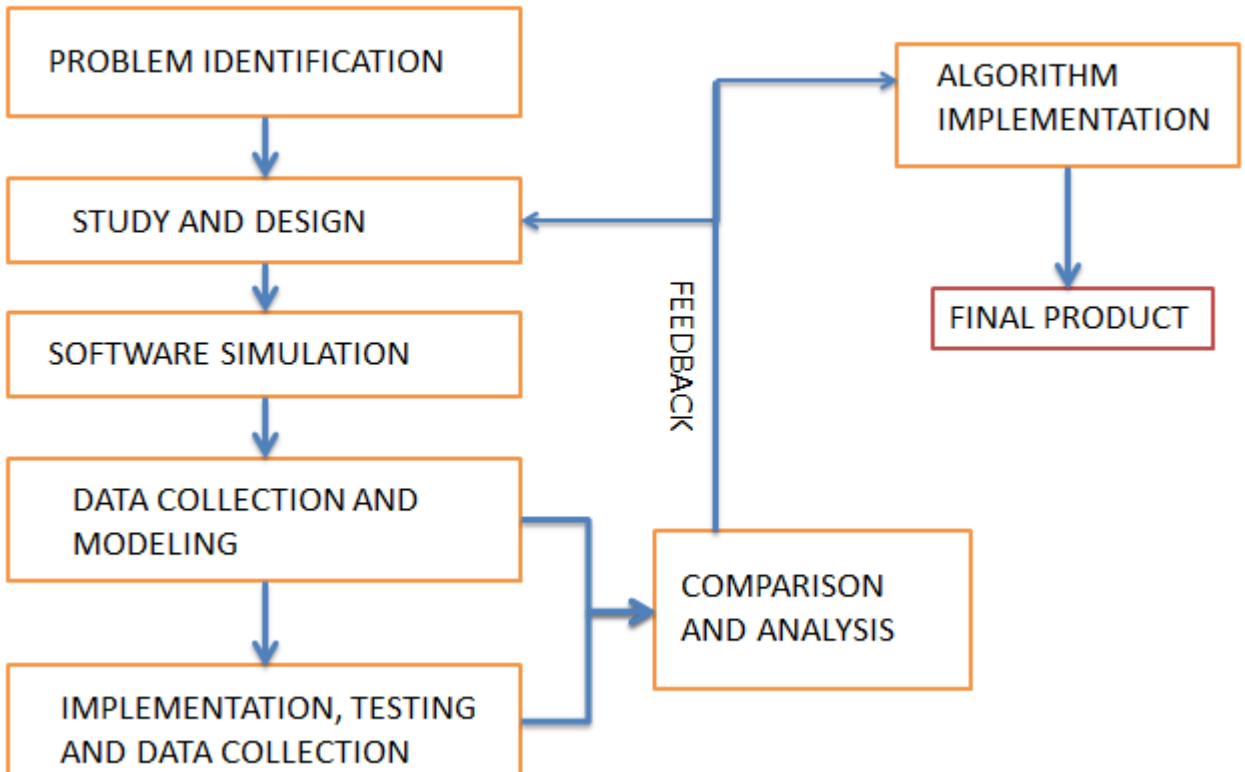


Figure 1.4: Phases of project

the sensor are optimized to get an operating frequency of 5.7 GHz. The ports are modeled with SMA connectors of 50Ω impedance and they are placed in contact with the microstrip line conductor. The sensor is designed on the FR4 substrate whose effective dielectric is constant at 5.7 GHz for 50Ω impedance. When the EM wave is launched from one port, most of the EM energy at the resonating frequency gets stored in the sensor structure, which remains available for interaction with the MUT resulting into a shift in the resonant frequency.

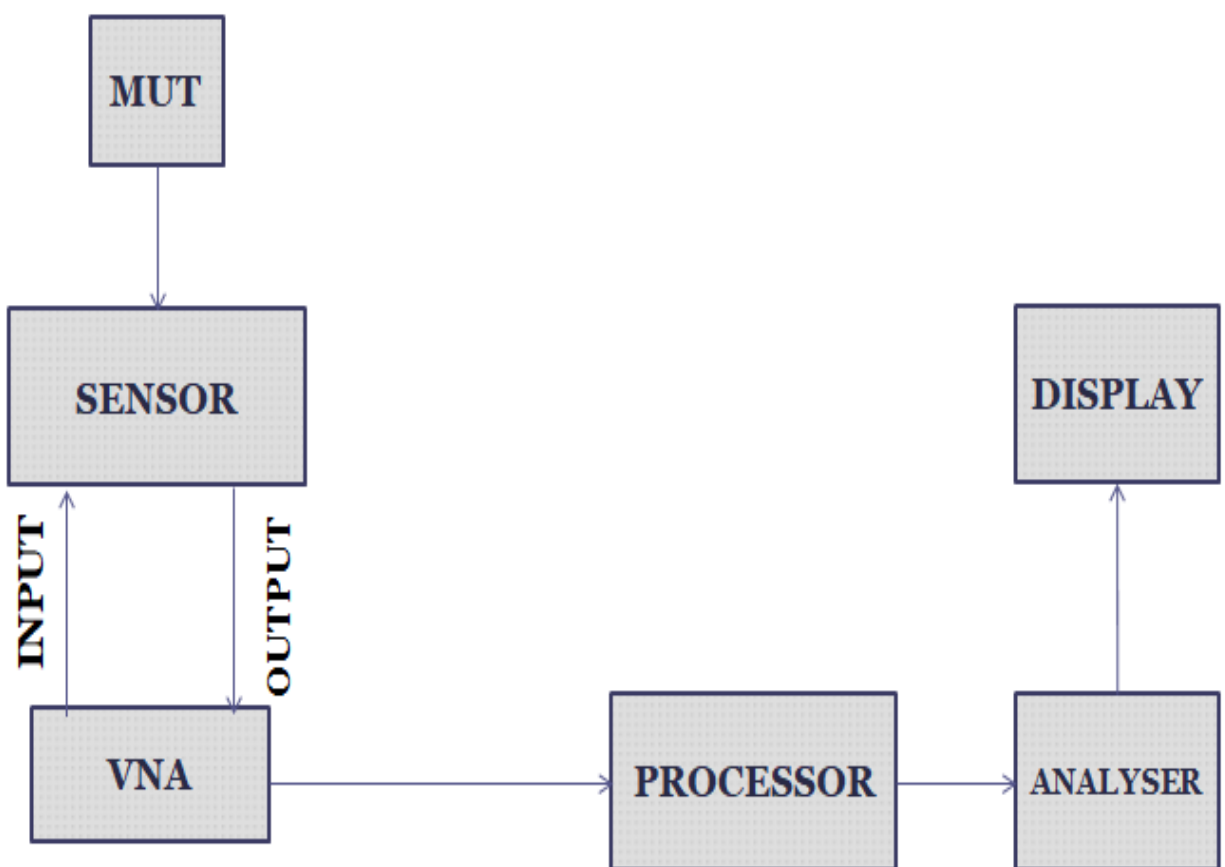


Figure 1.5: Proposed Model

Chapter 2

State Of Art

2.1 Food Adulteration and Evaluation

Food adulteration is a global concern and developing countries are at higher risk associated with it due to lack of monitoring and policies. However, this one of the most common phenomena that has been overlooked in many countries.

The term “quality evaluation” indicates obtaining meaningful information that can be used in making judgements, both positive and negative, about the degree of excellence of a food. “Non-destructive quality evaluation” indicates the analysis of a sample and the collection of its essential features in such a way that the physical and chemical properties of the sample are not altered. Non-destructive means no alteration or loss of the product, however, in relatively uniform products very small samples are commonly used that are representative of the bulk of the material (e.g., four 1 ml samples of oil from a 10,000 L tank; volume lost = 0.00004 percent of the total). These samples may or may not be altered during analysis and even when not altered, the material is seldom reintroduced into the bulk material. For practical purposes, the analysis can be considered non-destructive, since the samples typically represent only a minute fraction of the total amount of material (e.g., in liquids such as oils, juices, milk or

uniform solids such as ground meals). The number of samples required to accurately assess the presence of an adulterant depends upon the uniformity of the distribution of the adulterant or the percentage of adulterated product units in the bulk sample[3].

A major distinction between destructive and non-destructive procedures is that destructive analysis is typically used to identify an adulterant that has been added to or removed from a product and to assess the range in concentration. When possible, non-destructive methods are then developed for specific adulterants or a small group of similar adulterants. Non-destructive analyses tend to be less precise than traditional chemical analyses but have the advantage of speed, lower cost and often allow assessing each product unit rather than a sample of an entire volume. Assessing each product unit is important when the adulterant is not uniform, and each product unit must be individually assessed. This is especially critical when consumer health is imperiled by the adulterant. In such cases, a non-destructive means of monitoring each individual product unit is required[3].

2.2 Examples of Adulterated Foods

Properties of foods that were commonly altered included weight, volume, colour, odor, taste, composition, texture, geographical origin and cultivar designation. Adulteration of fruits and vegetables may occur through the addition of water, substitution of high-quality products with low-quality ones, sale of immature or overripe products, addition of antibiotics, preservatives, nitrates, transgenic vegetables or fruits and stimulators or inhibitors of product ripening. Products may be adulterated by immersing them in cold water to increase their weight and treatment of vegetables

with dyes (e.g., malachite green) which can contain pesticides and other chemical compounds.

Fruit juices can be adulterated by the addition of water, sugar, pulp, seeds or peel and alternative cheaper juices. Modern manufacturing technologies involve the addition of organic acids, beet and corn sugars, thickeners, artificial colouring and flavouring agents, preservatives, intensifiers of acidification, flavours and other less expensive juices. Orange juice can be adulterated with monosodium glutamate, ascorbic acid, potassium sulphate, corn sugar, grapefruit solids; pomegranate juice can be diluted with grape or pear juice, sugar, and high-fructose corn syrup.

Honey is a classic object of adulteration. Sucrose, sugar, glucose, partial invert cane and corn syrups and beet sugar, dextrin, starch, unripe honey, molasses, honeydew and artificial sweeteners have been intentionally added to natural honey. Some tested samples of honey did not contain pollen, but can be contaminated with heavy metals, pesticides and antibiotics.

Adulteration of olive oil usually is through dilution with alternative cheaper oils, such as sunflower, vegetable, hazelnut, corn, peanut, soybean, palm and walnut. In Spain in 1981-82, adulterated cooking oil resulted in 20,000 cases of illness and 12,000 hospital admission. Some 300 people died from what was called Toxic Oil Syndrome[4]. The cooking oil was illegally refined denatured rapeseed oil. Even 30+ years later the actual toxic agent in the oil has yet to be identified. Pet food from China in 2007 adulterated with melamine, a plasticizer which mimics high quality protein in routine quality control tests, resulted in thousands of dogs and cats dying and raised concerns about the safety of human foods imported from China[5]. An estimated 2.5 to 3 million people in the U.S. had consumed chickens that

had been fed feed containing contaminated vegetable protein from China.

2.3 Analytical Methods for the Detection of Adulteration

2.3.1 Analysis of the Headspace Gaseous Phase of Products

Headspace is the gas space or volume surrounding a sample in a closed but not necessarily sealed container. Headspace gas chromatography involves the analysis of volatile organic compounds (VOCs) in the headspace gas surrounding a product. There are two general sample collection techniques for gas chromatography: static headspace and dynamic headspace. In static headspace chromatography, the product is placed in a sealed glass container for a specific length of time. A sample of the headspace gas containing the VOCs that were given off by the product is withdrawn and transferred to the gas chromatograph for analysis[6] . Static headspace methods require minimal sample preparation.

VOCs emanating from fruits and vegetables can be classified according to their metabolic origin [e.g., terpenoids (e.g., sesquiterpenes and apocarotenoids), phenylpropanoids/benzenoids (e.g., eugenol, benzaldehyde), fatty acid derivatives (e.g., hexenal, hexenol) and amino acid derivatives (e.g., thiazole, 2- and 3-methylbutanal)]. From a chemical point of view, these VOCs can be divided into esters, alcohols, aldehydes, ketones, lactones, terpenoids and a cross-section of miscellaneous compounds. The following number of VOCs have been identified emanating from specific fruits and vegetables: strawberry–147, pear–303, tomato–more than 400, orange–203, banana–225, mango–273, apple–356 and grape–466[3].

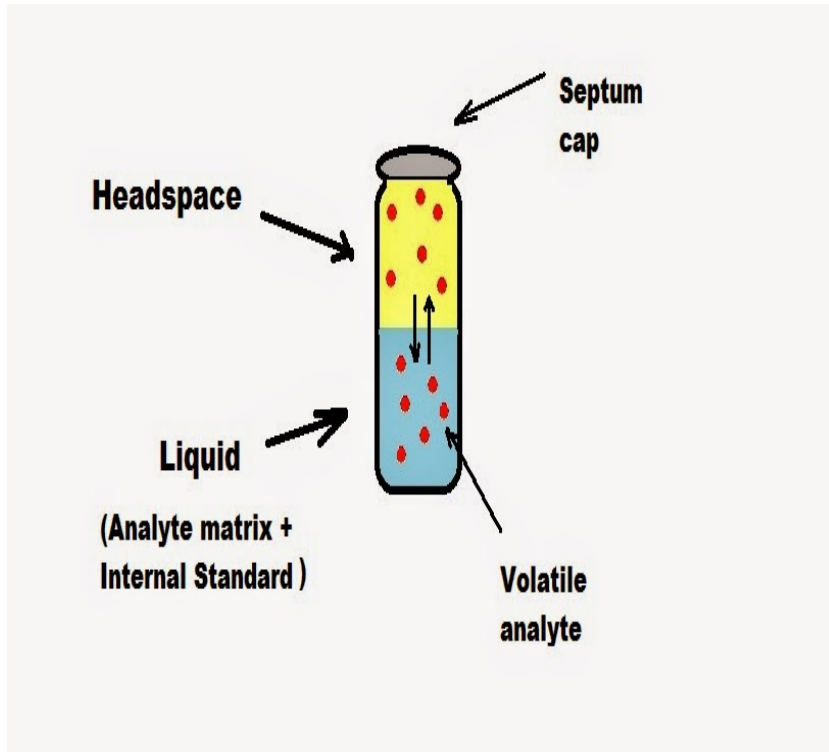


Figure 2.1: Headspace Gas Chromatography

2.3.2 Solid-phase Microextraction

SPME is a modified method of sample collection that can be used for the detection of VOCs in foods. This method is based on the application of a fused fiber coated with a polymer that traps volatile analytes (VOCs) emanating from a sample. An equilibrium between the sample, headspace above the sample and the fiber is established. The analyte is deposited on the fiber which is then transferred to the injection port of a gas chromatograph equipped with mass spectrometer detector for analysis. When the fiber is inserted into the injection port, the trapped volatiles are thermally released and subsequently separated on the GC column.

A combination of SPME, gas chromatography and chemometric data analysis allowed differentiating among pure strawberry samples (*Fragaria ananassa* Duchesne) and strawberry samples adulterated with 10, 40 and 70 percent (v/v) apple puree[20]. Another example of detecting adulteration of

honey with thyme oil demonstrated the effectiveness of the SPME-GC/MS procedure which is based on the analysis of specific volatiles such as thymol and carvacrol[19]. The authors demonstrated that adulterated honey had an intense thyme aroma without the characteristic honey flavour; they proposed using the presence of the volatile 3,4,5-trimethoxybenzaldehyde as a possible marker of honey adulteration.

Solid-phase microextraction is fast, simple, fairly sensitive and can be used without solvents, eliminating the need for environmental hazards. The disadvantages of SPME fibers include the high selectivity of the fibers for specific chemicals, lack of robustness and low reproducibility of results due to ageing of the fiber.

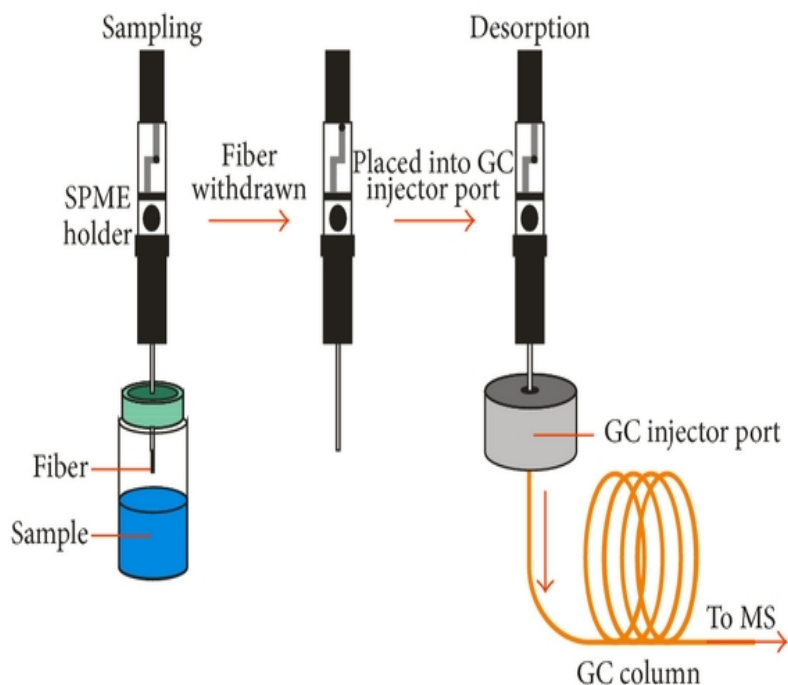


Figure 2.2: Solid-phase Microextraction

2.3.3 Mass Spectrometry

Mass spectrometry is an analytical technique for the separation of ionized atoms and molecules according to their mass-to-charge ratio using electrical and magnetic fields in a vacuum and identifying the composition and structure of the chemicals.

A typical mass-spectrometer contains an ion source that transforms neutral molecules of a sample into ions, a mass analyser that separates ions by their mass and charge in applied electric and magnetic fields and a detector that provides a qualitative and quantitative estimation of sample compounds. There are two principal types of mass- spectrometers: a sector field mass analyser that measures the mass-to-charge ratio of charged particles that are accelerated by an electric field and are separated based on their mass and charge in a magnetic field and a quadrupole mass analyser that separates the ions according to their mass-to-charge ratio, which is determined by the trajectories of the ions under the influence of an electric field[3].

Mass spectrometers are characterized by high sensitivity and accuracy; at the same time, it should be noted the need for a trained operator and the relatively high cost of the equipment. Very often, mass spectrometry is used in combination with other methods, extending the analytical possibilities.

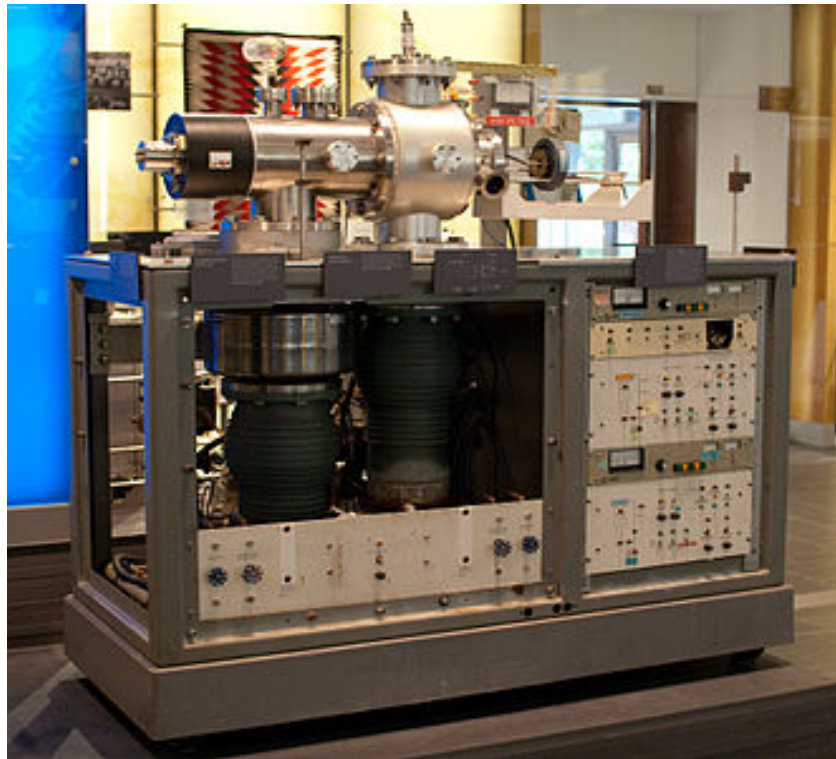


Figure 2.3: Quadrupole Mass Spectrometer

2.3.4 Electronic Nose and Electronic Tongue

A device that can be used to detect odors that are often significant components in the overall flavour of food products is called an electronic nose (eNose). It consists of a large array of chemical sensors, a detection system and a computing system. Sensors can be fabricated using different types of polymers, metal oxide semiconductors, metal oxide semiconductor field effect transistors, piezoelectric crystals, quartz crystal microbalance and surface acoustic wave transducers.

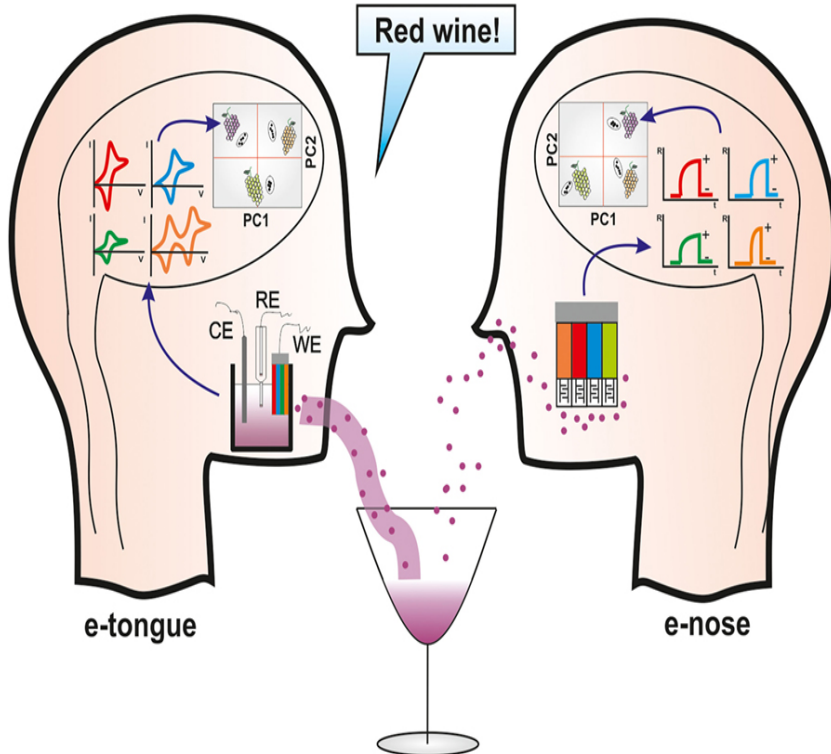


Figure 2.4: Electronic Nose and Electronic Tongue

The principle of operation of an eNose is based on the exposure of the sensor surface to an odor (flavour) which is composed of molecules of different sizes and shapes. When a certain polymer film receives a specific molecule, the film begins to swell. The process of film swelling causes a corresponding change in the electrical conductivity of the film that is assessed by the detector. The interaction of flavour components with the sensor array allows detecting a pattern using software recognition.

An eNose system, which was based on the application of 10 metal oxide semiconductor sensors, was used to generate a pattern of the volatile compounds present in samples of sesame oil. Excellent results were obtained in the prediction of the percentage of adulteration in the oil using back propagation neural networks and general neural network regression[7].

The electronic tongue (eTongue) is an instrument that detects dissolved

organic and inorganic compounds, some of which are responsible for taste. It contains several sensors (electrodes) that are characterized by differing spectra of reactions and the response is based on the chemical modification of these voltammetric electrodes. The combination of all responses produces a specific fingerprint similar to the human taste reception. Several approaches for the qualitative determination of adulteration levels have been performed using this instrument. It has been used successfully for the detection of fraudulent red wines created through the addition of a range of adulterants. In this case, the sensor array that was used consisted in two families of electrodes, i.e., phthalocyanine-based carbon paste electrodes (CPEs) and electrodes covered with a conducting polypyrrole treated with a range of counter ions.

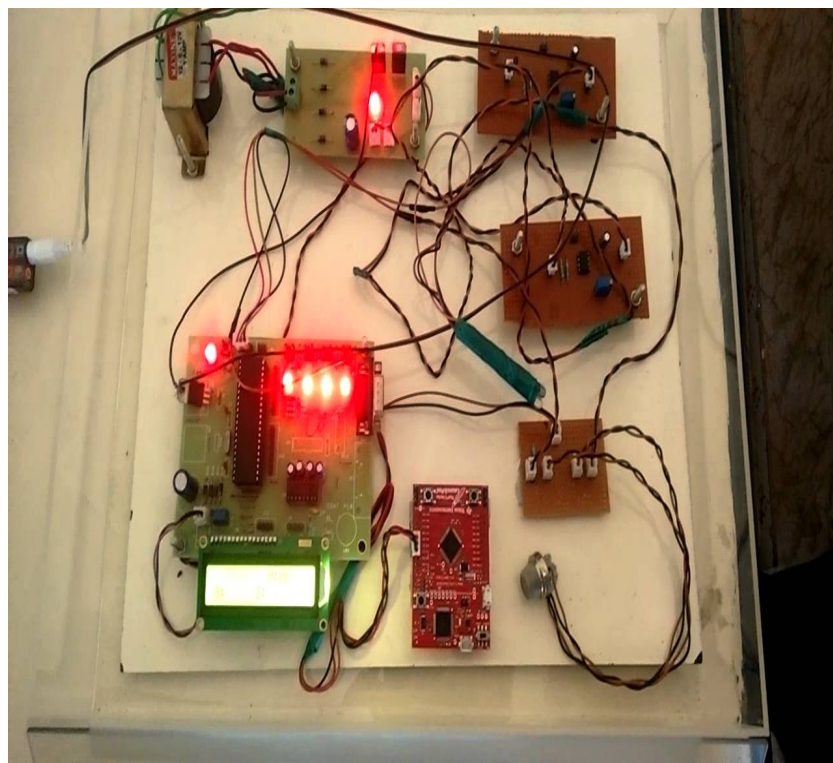


Figure 2.5: Electronic Nose and Electronic Tongue Circuit

2.3.5 Fourier Transform Infrared Spectroscopy

Fourier transform infrared spectroscopy (FTIR) is an analytical system that is used to convert raw data into the actual infrared spectrum of a sample through such mathematical process as Fourier transform that converts an amplitude-time spectrum to an amplitude-frequency spectrum or vice versa. This analytical technique is based on the measurements of the temporal coherence of a radiative source, using time-domain measurements of the electromagnetic radiation or other types of radiation.

One of the main devices for measuring the temporal coherence of light is the Michelson or Fourier transform spectrometer which consists of a light source, beam splitter, movable and fixed mirrors and detector.

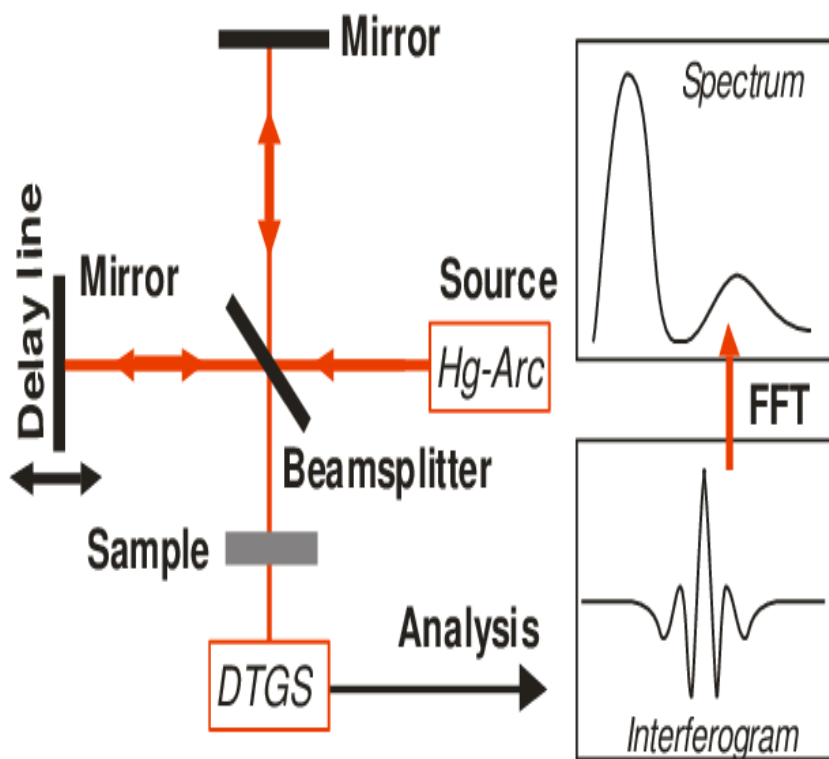


Figure 2.6: Fourier Transform Infrared Spectroscopy Setup

FTIR spectroscopy was successfully applied for adulteration detection in pure pomegranate juice concentrate in which grape juice was added. Three

types of fruit purees namely strawberry, raspberry and apple were successfully classified with 100 percent success using FTIR in combination with discriminant analysis. It was also possible to classify the source if the purees were made from fresh or freeze-thawed with 98.3 percent success for strawberry and 75 percent for raspberry. FTIR spectroscopy was also used to develop a model that predicts the percent composition of Concord grape juice. The model predicted Concord concentrations in samples ranging from 50 to 100 percent concord juice with a standard error of prediction of 5.6 percent. This results suggesting that the feasibility of using FT-IR coupled with chemometrics as a production-scale tool for authentication claims of Concord in grape juice blends, protecting consumers and businesses against deceptive labeling.

If the source is monochromatic and the movable mirror is moved at a constant rate, the detector signal oscillates with a single frequency. The radiant power can be recorded as a function of time as the cosine oscillation (time domain) or as a function of frequency as the spectral line (frequency domain). The plot of the output power from the detector versus the mirror displacement is called an interferogram. If the source is polychromatic, each input frequency can be considered to produce a separate cosine oscillation; the resulting interferogram is a summation of all cosine oscillations caused by all frequencies in the source. The recorded signal is mathematically manipulated using a Fourier transform technique to produce a spectrum that can be used to identify specific contaminants and their concentrations[3].

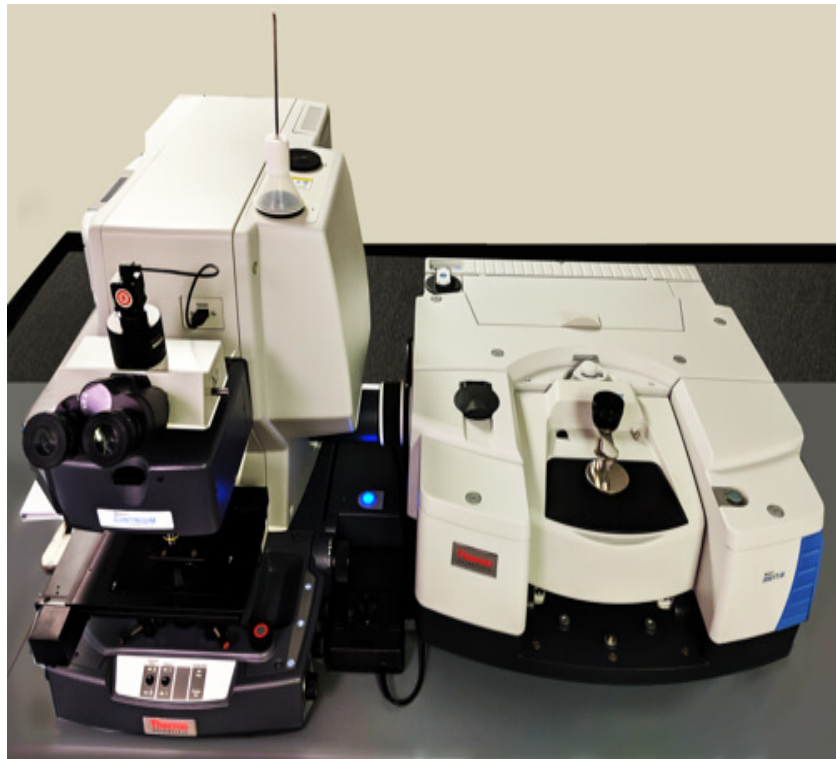


Figure 2.7: Fourier Transform Infrared Spectrometer

2.3.6 Nuclear Magnetic Resonance Spectroscopy

Nuclear magnetic resonance spectroscopy (NMR spectroscopy) is a spectroscopic technique that is based on the analysis of the magnetic properties of atomic nuclei that possess spin. Certain nuclei have quantum number $I \neq 0$ (for example, nuclei of organic molecules, such as ^1H , ^{13}C , ^{19}F and ^{31}P have spin of $I = 1/2$). A spinning charge generates a magnetic field, known as a magnetic moment which is proportional to the spin. When a nucleus is located in a static magnetic field B_0 , two spin states occur, $I = +1/2$ and $I = -1/2$. The magnetic moments of both states are aligned with the external field ($I = +1/2$) and opposed to the external field ($I = -1/2$).

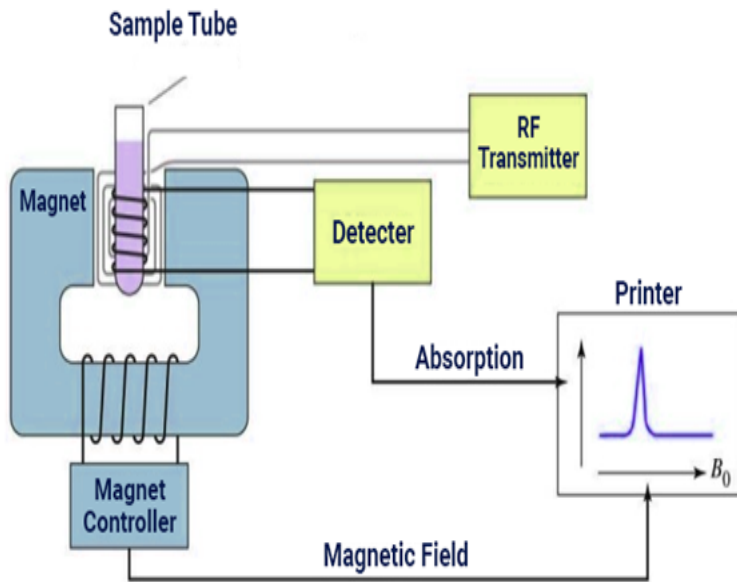


Figure 2.8: Nuclear Magnetic Resonance Spectroscopy

The adulteration of virgin olive oil with a wide range of seed oils was detected at level as low as 5 percent by means of application of combined ^{31}P and ^1H NMR spectroscopy and with multivariate statistical analysis, which was performed on 13 compositional parameters derived from the spectra[17]. In the Italian oenological industry, a regular practice used to naturally increase the colour of red wines consists in blending them with a wine very rich in anthocyanins, namely Rossissimo. In the Asian market, on the other hand, anthocyanins extracted from black rice are frequently used as correctors for wine colour. This practice does not produce negative effects on health; however, in many countries, it is considered as food adulteration. Ferrari et al., [18] tested FT-NIR and ^1H NMR spectroscopy methods and found that ^1H NMR spectroscopy can successfully discriminate wines added with the blending wine Rossissimo from wines adulterated with anthocyanins extracted from black rice to increase their Color Index.



Figure 2.9: Nuclear Magnetic Resonance Spectrometer

2.3.7 Raman Spectroscopy

When light passes through a particular material it may be absorbed, scattered or else simply pass through unobstructed if the photons do not interact with the molecules of the matter. When the energy of the incident photon corresponds to the energy gap between the ground state of a molecule and an excited state, the photon may be absorbed and the molecule promoted to the higher energy excited state. This phenomenon of energy absorption is used in a wide range of absorption spectroscopic techniques such as UV, VIS, NIR and IR spectroscopy. It is also possible for a photon to interact with a molecule and scatter (deflect from the original direction of propagation of incident light) from it. For scattering of photons by a molecule, it is not necessary for the photon to have an energy that matches the two energy levels of the molecule. Such scattered photons can be detected by collecting light at an angle to the incident light beam.

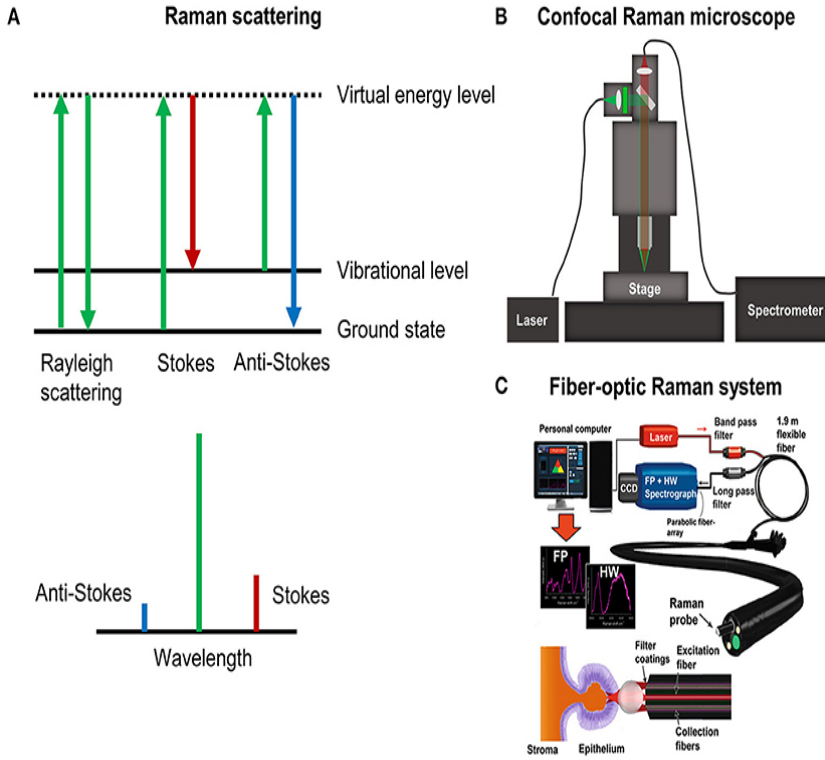


Figure 2.10: Raman Spectroscopy

Raman spectroscopy has several advantages over mid-IR and NIR spectroscopy. Spectra can be obtained with little or no sample preparation therefore, it can be used for non-destructive testing of materials, often those inside glass or plastic containers[8]. Since water is a weak scatterer, materials with high moisture levels or aqueous solutions can be easily analyzed using Raman spectroscopy. Raman spectroscopy can be used to measure bands of symmetric linkages which are weak in an infrared spectrum. Raman spectroscopy can also be used for both qualitative and quantitative applications. As in infrared spectroscopy, band areas are proportional to concentration, making Raman spectroscopy open to quantitative analysis. In fact, because Raman bands are inherently sharper than their infrared counterparts, isolated bands are often present in the spectrum for more straightforward quantitative analysis.

Because of the above mentioned advantages, Raman spectroscopic methods have been developed for rapid non-destructive analysis and screening of adulterants in numerous agricultural and food products. Zhang et al.,[9] used SERS to detect melamine in liquid milk with minimal sample preparation. The limit of detection by this method was 0.01 microgram per ml for melamine standard samples and 0.5 microgram per ml of melamine in liquid milk. The test results for SERS were very precise and as good as those obtained by liquid chromatography/tandem mass spectrometry. The method was simple, fast (only requires about 3 min), cost effective and sensitive for the detection of melamine in liquid milk samples. Therefore, it is more suitable for the field detection of melamine in liquid milk.

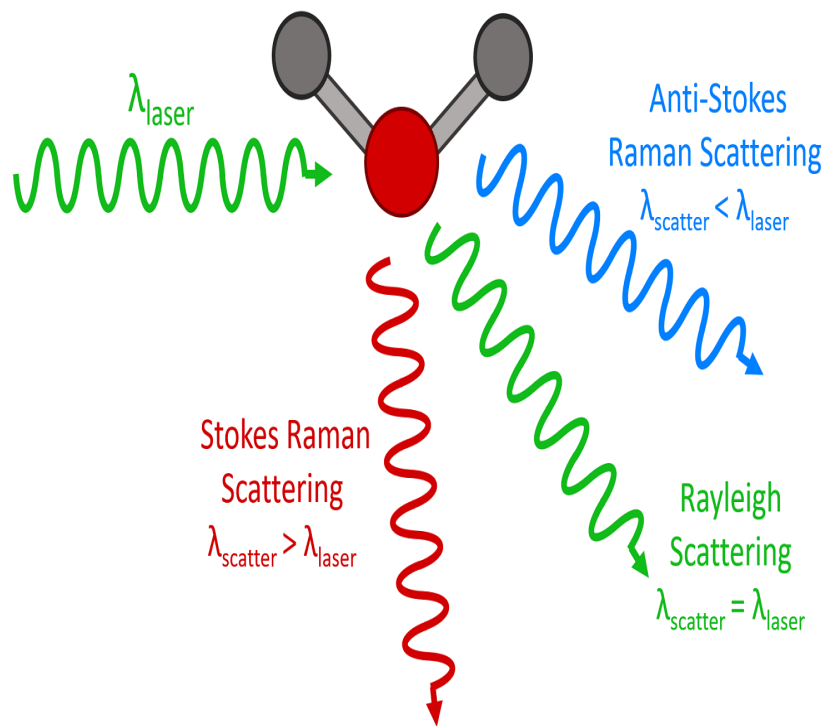


Figure 2.11: Raman Scattering

2.3.8 Infrared Spectroscopy

Adulteration level of meat products, especially minced beef, is estimated using non-destructive spectroscopic methods. Mixtures of minced beef

adulterated with turkey meat in the range 5–50 percent (w/w) were prepared and analyzed through the methods of UV-visible, near infrared (NIR) and mid infrared (MIR) spectroscopy[10]. The best results were obtained with NIR and MIR spectroscopy.

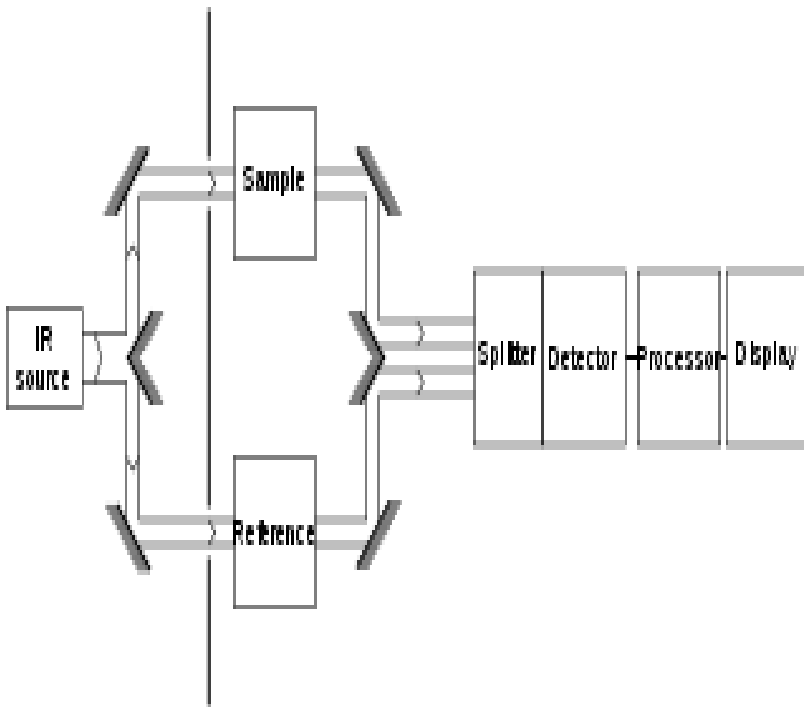


Figure 2.12: Infrared Spectroscopy

Methods of visible and short wave near infrared (VIS/SW-NIR) spectroscopy were used for the rapid, non-destructive detection of beef adulteration. This spectroscopic technique was applied to the samples of pure minced beef, pork and beef liver, beef and pig fat trimming as well as the mixture samples in the form of minced beef adding different proportion of others, respectively. The results demonstrated that the VIS-SW-NIR spectroscopy can be used to detect and classify the amount and level of adulterants added to the minced beef with acceptable precision and accuracy. Likewise, the results of application of near infrared spectroscopy (NIRS) for detecting and quantifying different adulterants (pork, fat

trimming and offal) in fresh minced beef demonstrated good performance .

The adulteration of pork in beef meatball was studied by Rohman et al[11]. The application of Fourier transform infrared (FTIR) spectroscopy and partial least square (PLS) calibration made it possible to distinguish pork fat (PF), beef fat (BF) and their mixtures in meatballs.

Ding and Xu[12] developed a NIR spectroscopic technique to detect beef hamburgers adulterated with 5–25 percent mutton, pork, skim milk powder or wheat flour with an accuracy up to 92.7 percent. The accuracy of detection increased with the increase of adulteration level. When an adulterant was detected, the adulteration level was further predicted by calibration equations. The established calibration equations for predicting adulteration levels with mutton, pork, skim milk powder and wheat flour had standard errors of cross-validation of 3.33, 2.99, 0.92 and 0.57 percent.

2.3.9 High-Performance Liquid Chromatography

The distinguishing feature of high-performance liquid chromatography (HPLC) is the application of high pressure (400 bar) and a fine-grained sorbent (a granular material made of solid particles 3-5 micrometers in size). It allows separating a complex mixture of substances quickly and completely (average analysis time is 3-30 min) with high resolution.



Figure 2.13: High-Performance Liquid Chromatography

HPLC is preferred for analysis of liquid samples; and it can be useful for separation of organic compounds independent of their polarity and volatility. The literature highlights the possible applications of HPLC for the quality evaluation of fruits and vegetables and detection of their possible adulteration. In general, this method can be used for analysis of pesticide residues, flavours, organic acids, mycotoxins, antibiotics, additives, food colours, carbohydrates, proteins, pigments, dyes and different adulterants in foods[13].

HPLC analysis of flavanones such as naringin, neohesperidin and neoeriocitrin that are present in bergamot fruit (*Citrus bergamia* Risso and Poit.) juice and essentially absent in lemon juice can be used for detecting the fraudulent addition of bergamot juice to lemon juice.

Artificial food dyes are added to a number of food products such as fruit

snacks and juices; however some of these dyes can cause cancer, allergic reactions and hyperactivity. HPLC is an effective method of identifying synthetic dyes, determining if synthetic dyes are present in a food and whether they are permitted.

Argan oil obtained from the argan fruit (*Argania spinosa* (L.) Skeels) is very popular due to its beneficial dietary properties and its apparent reduction in the risk of cardiovascular disease and cancer. Triacylglycerols were used as indicators of argan oil adulteration with vegetable oils such as sunflower, soybean and olive. These compounds can be readily separated by high-performance liquid chromatography and measured using evaporative light scattering detection[14].

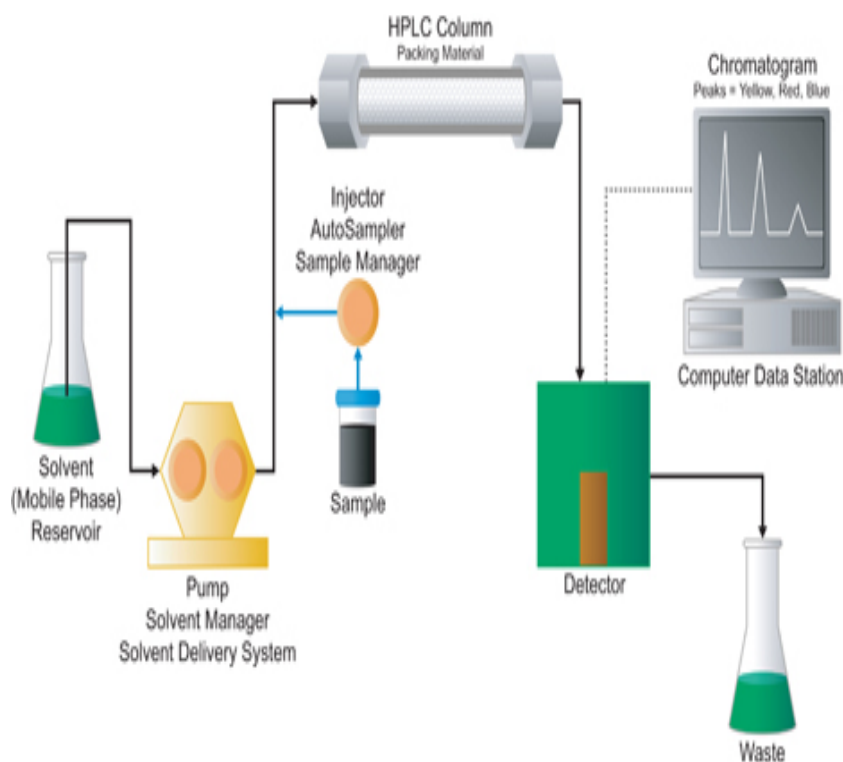


Figure 2.14: High-Performance Liquid Chromatography Setup

2.3.10 Hyperspectral Imaging

Hyperspectral imaging is rapidly gaining ground as a non-destructive, real-time detection tool for produce quality and safety assessment. Hyperspectral imaging could be used to simultaneously obtain large amounts of spatial and spectral information on the objects being studied. Hyperspectral techniques are used to detect pathogens, defects and contaminants and also to evaluate certain quality attributes of fruits and vegetables. Since the quality attributes of fruit and vegetable products show significant variation within the product unit, hyperspectral techniques that can encompass spatial variability may be more suitable for such products. Therefore, these techniques may be useful to detect intentional adulteration or prevent unintentional contamination of produce with poor quality product units.

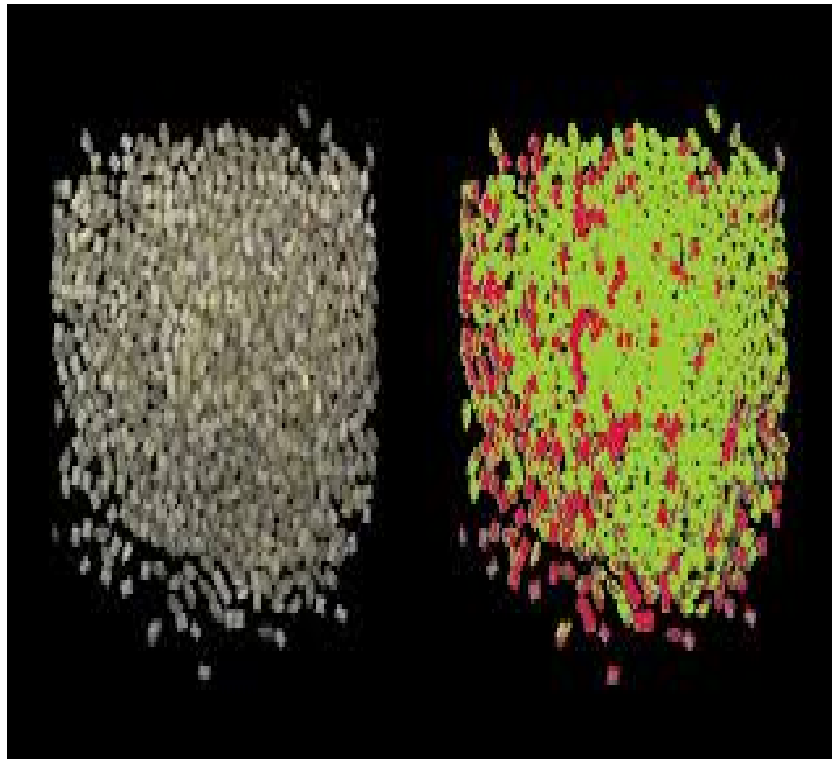


Figure 2.15: Hyperspectral Imaging

Bruising is the most common type of mechanical damage affecting fresh

horticultural produce. It reduces quality to the consumer and income to fruit and vegetable industries. Bruising can occur during harvest and at all stages of postharvest handling, especially during packhouse operations, transport and storage, and is one of the major physical defects contributing to downgrading and postharvest losses in fresh horticultural produce. Novel and emerging non-invasive technologies for bruise measurement of fresh horticultural produce include NIR spectroscopy, hyperspectral imaging, thermal imaging and nuclear magnetic resonance imaging[15].

The early detection of bruises in apples was studied using a system that included hyperspectral cameras equipped with sensors working in the visible, near-infrared (400-1000 nm) and short wavelength infrared (1000-2500 nm) ranges and a thermal imaging camera in the mid-wavelength infrared (3500-5000 nm) range. Principal component analysis (PCA) and minimum noise fraction (MNF) analyses of the images that were captured in particular ranges made it possible to distinguish between areas with defects in the tissue and sound tissue. Fast Fourier analysis of the image sequences after pulse heating of the fruit surface provided additional information not only about the position of the area of damaged tissue but also about the depth of damage. Results confirmed that broad spectrum range (400–5000 nm) fruit surface imaging can improve the detection of early bruises of varying depths.

Lee et al.[16] used hyperspectral imaging in the 950–1650 nm range for detecting bruise damage underneath the surface of pears. A classification algorithm based on F-value was applied for analysis of the image to find the optimal waveband ratio for discrimination between bruised and sound surfaces. The results demonstrated that the best threshold waveband ratio for detecting bruises had an accuracy of 92 percent, illustrating that the

hyperspectral infra-red imaging technique could be a potential detection method for pear bruising.

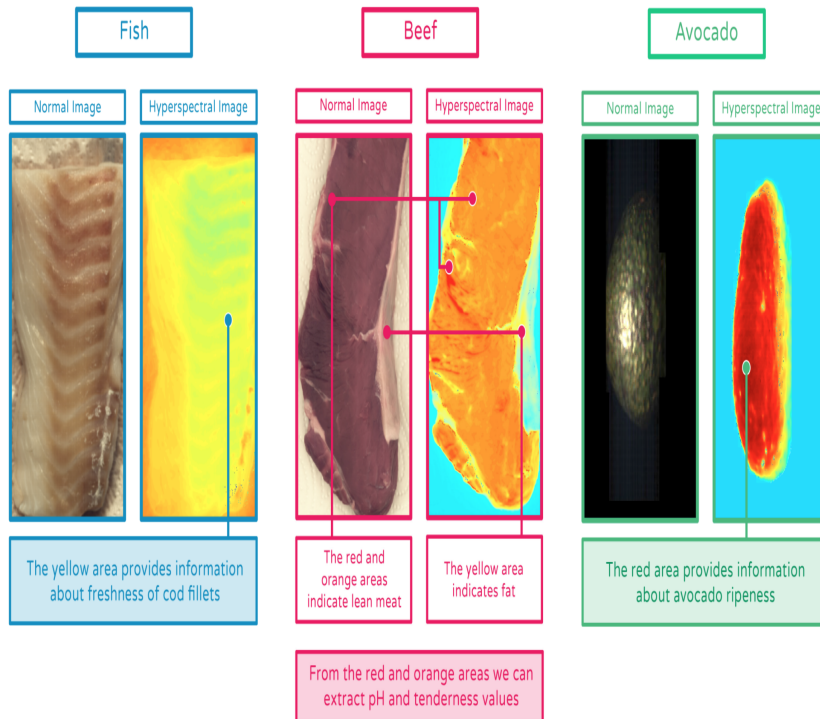


Figure 2.16: Hyperspectral Imaging in Foods

2.4 Detection of Food Adulteration using Microwave Antenna over Conventional Methods

This is one of the most innovative solution to the problem of food adulteration. In this method very fast emerging technology of microwave antennas are used. There are many disadvantages of conventional methods of food adulteration detection which can be addressed using microwave detection using antenna.

The main disadvantage of Headspace Gas Chromatography method is associated with the low concentrations of the compounds in the sample that can make detecting and identifying some potentially critical quality components difficult. The disadvantages of Solid-phase Microextraction

(SPME) fibers include the high selectivity of the fibers for specific chemicals, lack of robustness and low reproducibility of results due to ageing of the fiber. Mass Spectroscopy and Raman Spectroscopy method needs a trained operator and Mass Spectroscopy has a relatively high cost of the equipment. Electronic Nose and Electronic Tongue Method needs a large number and varieties of sensors making the method expensive and complex. Disadvantages of Nuclear magnetic resonance spectroscopy are the high cost due to the need for a strong liquid helium-cooled superconducting magnet; measurements are time consuming and not very sensitive; and the sample should be dissolved in a solvent. There are many disadvantages of conventional methods like being destructive testing and also some are time consuming and not very efficient and some has limited application only.

Almost all of the above mentioned problems can be addressed using microwave antennas for food adulteration detection. This is a simple and reliable method of adulteration detection. This has huge application and can be used to detect impurities in almost all food items rather than limited application as in conventional testing methods and is robust. It is a non-destructive testing method. Also for the evaluation and analysis of the contaminant we do not need expert consultation as in conventional methods. It is a very cheap method. When there is an impurity in food item, there will be a slight change in its resonance frequency. The microwave antenna captures this shift and finds out the impurity and its concentration in the food. The antenna is very sensitive and hence can give accurate results. This method also has high reproducibility which makes the technique more reliable. It can detect impurities rapidly. It is not complex and is very easy to use. We can detect impurities even from a small quantity or lower concentration of the food. This method can hence be called a breakthrough in the food and safety sector.

Chapter 3

Working

This chapter explains the theory, design, simulations and modelling of the sensor antenna.

3.1 Theory

The non-destructive testing and the lesser volume of sample for testing makes this approach of testing food items very popular. There are different RF material characterization techniques available, which can be divided under the non-resonant and resonant methods. The non-resonant methods are normally used for wide-band characterization of samples with moderate accurate results and hence the resonant methods are preferred over non resonant methods for obtaining accurate results over narrow band of operation.

Among the RF resonant methods, the food material characterization can be performed either using the cavity resonators or with the help of planar resonant sensors. Planar resonators are preferred over the cavity resonators as they are of low cost, can be easily fabricated and can be easily integrated with other microwave circuits.

For the implementation of planar resonant methods, various resonant structures such as combination of series resonators (SR), inter digital

capacitor (IDC), split ring resonator (SRR), complementary split ring resonator (CSRR) etc. have been used. Additionally, the planar sensors are fabricated using both the micro strip and the coplanar waveguide technologies.

Among these different resonant structures, the IDC and some specialized resonators are fabricated on the main micro strip line. On the contrary, in the case of the SRR and CSRR structures, the resonant structure is coupled to the micro strip line either electrically or magnetically depending upon the orientation of the resonator with the micro strip line[21]. Since the IDC type resonators are fabricated on the main transmission line using the micro strip technology, they are easy to get fabricated and provide reasonably higher amount of sensitivity. Recently, the microwave resonant sensors have been used to estimate the permittivity for different polar and non-polar organic chemical solvents, for detection of water level in petroleum products and for detection of adulteration in common edible liquids[22].

A planar resonant RF sensor based on a generalized IDC like structure is proposed for liquid characterization. The proposed structure is etched on the main micro strip line for getting the maximum sensitivity and the basic design is carried out using ANSYS HFSS 15.0.3, a Numerical model is proposed using the curve fitting tool in Microsoft Excel. The developed numerical model is used to calculate the real and imaginary parts of the complex permittivity of various edible oils. Finally, the proposed sensor is used for finding the percentage adulteration in the standard edible oils.

3.2 Principle

Most of the planar resonant RF sensors are based on the electromagnetic (EM) field perturbation approach. Since the electric field in the resonant

structure is mainly responsible for the characterization of material under test (MUT), the MUT is kept in close contact with the resonant structure of the sensor. The electric field confined to the resonant structure of the RF sensor interacts with the MUT at the resonant frequency. The loading of MUT on the sensor changes the effective capacitance of the equivalent circuit of the resonant structure, which causes a shift in resonant frequency. This resonant frequency shift of the sensor is mainly attributed to the real part of the complex permittivity of the MUT. Similarly, the changes observed in the quality factor of the RF sensor under loaded condition are pertained to the loss associated with the MUT.

The ports are modelled with SMA connectors of 50 ohm impedance, and they are placed in contact with the micro strip line conductor. The sensor is designed on the FR4 substrate whose effective dielectric constant is 3.5 at 5.7 GHz for 50 ohm impedance. When the EM wave is launched from one port, most of the EM energy at the resonating frequency gets stored in the sensor structure, which remains available for interaction with the MUT resulting into a shift in the resonant frequency. Fig. 3.1 and 3.2 shows the proposed sensor structure with optimized values of different dimensions and enlarged view of the resonant structure.

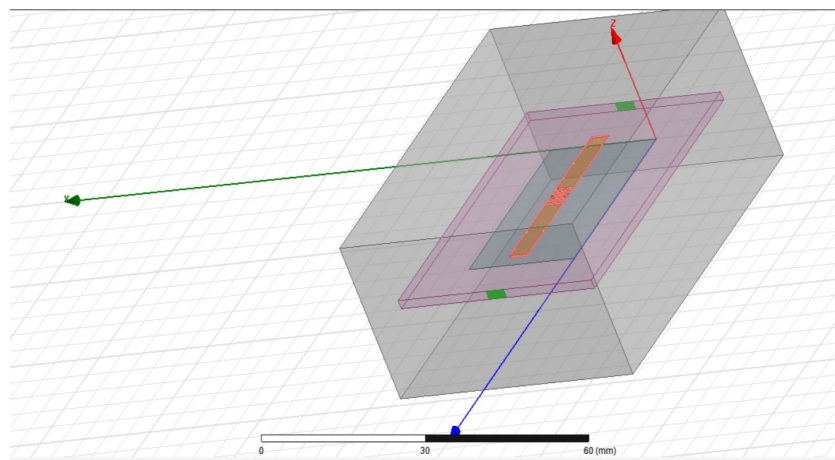


Figure 3.1: Simulation setup in HFSS

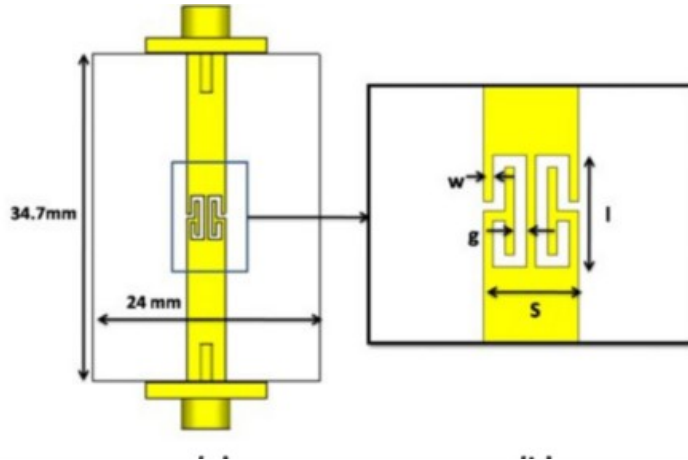


Figure 3.2: Antenna dimensions

3.3 Structure and Design

The structure was obtained by using a tool in CST Microwave Studio called full wave electromagnetic solver. The proposed sensor is a uniplanar IDC structure. The principle of such a sensor is based on the interactions between the electromagnetic field and the fluid under test. When unfilled (e.g., when no fluid is introduced in the channel), the stop band resonator is characterized by parameters such as resonant frequency, associated transmission loss and quality factor. When a fluid characterized by its complex permittivity is inserted in the microfluidic channel, the above listed parameters are modified and thus contain information relative to the fluid under test.

The characterization of the complex permittivity is based on the quantification of the resonant frequency and peak attenuation shifts due to the fluid filling. Any resonant structure can be implemented by using coplanar waveguide (CPW) and slot lines. As shown in the structures from the Fig 3.3 resonant structures can be implemented. Several variants of these types can be used in practice to achieve specific circuits.

In order to understand the electromagnetic behaviour of these resonators, it

is necessary to study their response as a function of frequency so as to better understand their effect on the performance of filters. Therefore, a rigorous space-domain integral-equation (SDIE) method[23] solved by the method of moments (Galerkin's technique) in conjunction with simple transmission-line theory is applied to analyse the structures.

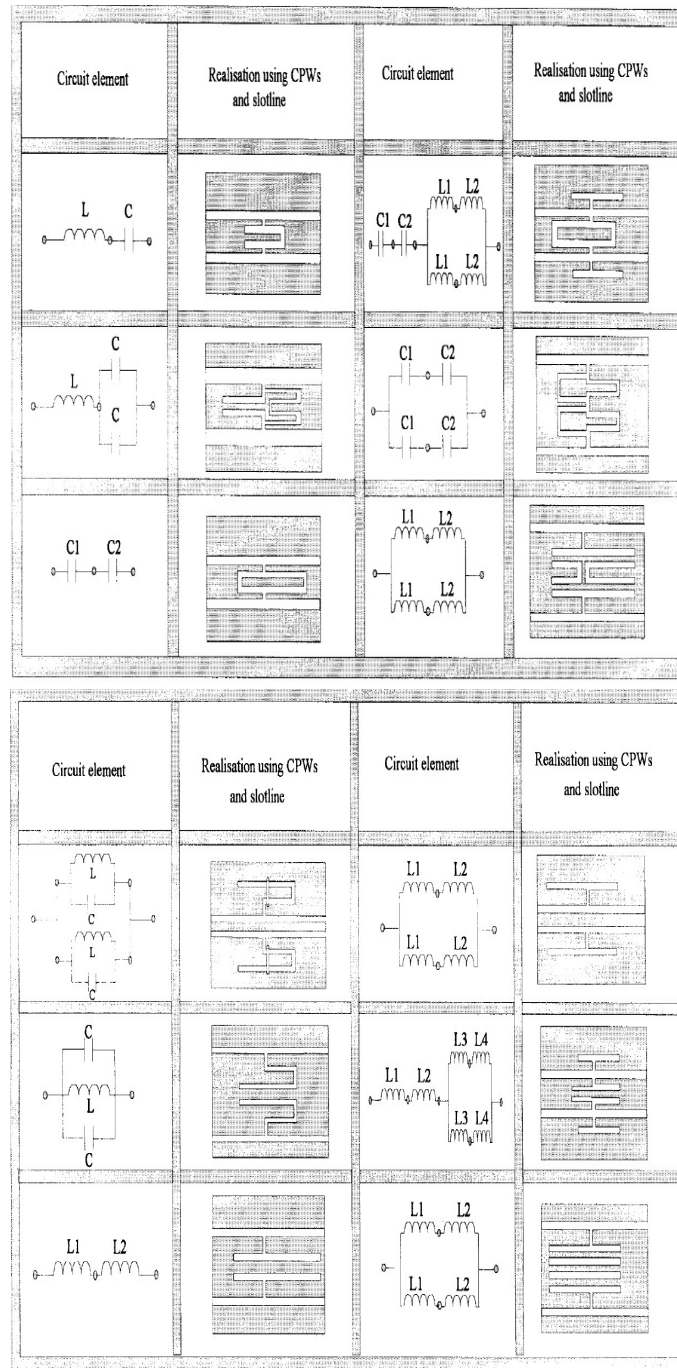


Figure 3.3: Implementation of resonant structures using CSW and slotted lines

3.4 Simulation

Simulation for this project was mainly done in ANSYS HFSS 15.0.3. Initially a model was created specifying materials for each sub structure in the structure. HFSS contains two types of structures; sheets (2D) and Boxes (3D). Initially all substructures were created as boxes and the material of the patch was specified as copper. Materials can be specified only for boxes in HFSS. Sheets were not used in the initial structure. This caused a great deflection in the resonant frequency. So we switched to sheets and specified a Perfect E boundary condition. There are several boundary conditions in HFSS like Perfect E and Perfect H. Perfect E makes the material exhibit properties of a conductor which can be approximated to that of copper. The simulation results almost matched with the resonant frequency (5.7GHz).

An air box surrounding the antenna structure was also created, which had about double the dimension of the antenna structure and extending in all directions. The position of the MUT was decided by plotting the E field intensity in the resonant structure as shown in Fig 3.4. Thus the ideal position for the MUT was decided to be at the centre of the antenna.

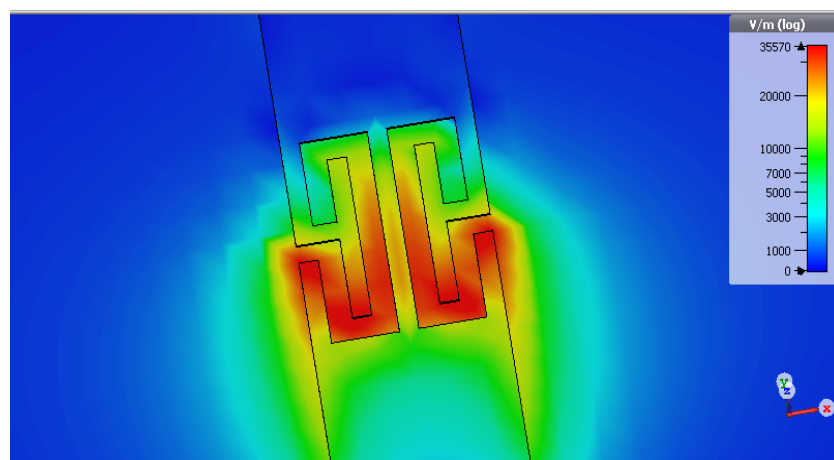


Figure 3.4: Electric field intensity distribution

Three cases were taken to determine the exact position of the MUT:

3.4.1 CASE 1

Firstly the MUT with relative permittivity 2.2 was placed below the sensor antenna as shown in figure 3.5 and the resulting S21 output is shown in figure 3.6, from this we can infer that there is no notable change in the resonant frequency obtained, so the sensor antenna parameters are not affected by the properties of MUT.

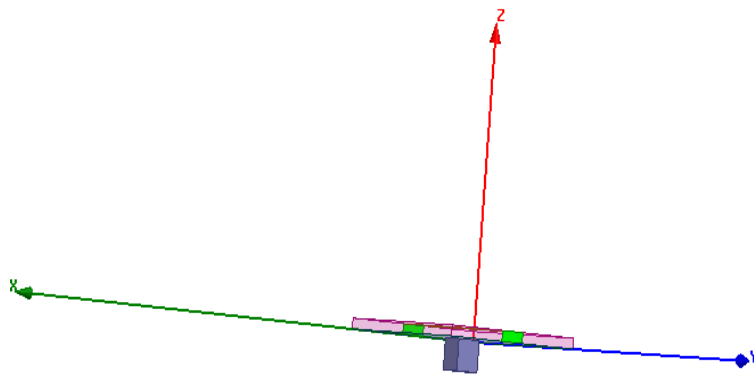


Figure 3.5: Simulation setup for MUT below sensor

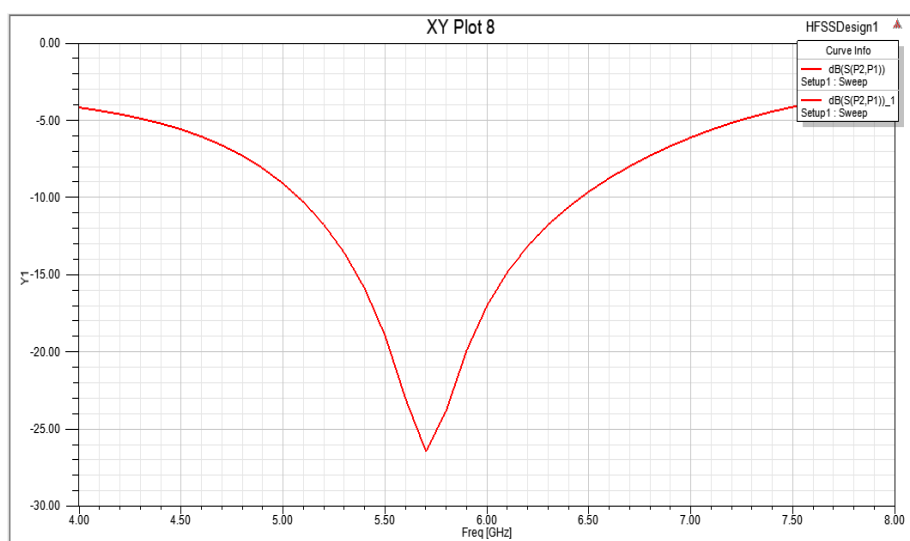


Figure 3.6: S21 for MUT below sensor

3.4.2 CASE 2

After finding the position a suitable height above which MUT must be placed should be obtained, for this the height above which MUT was kept above the antenna was varied. Figure 3.7 shows MUT placed 1mm above antenna and figure 3.8 gives corresponding resonant frequency.

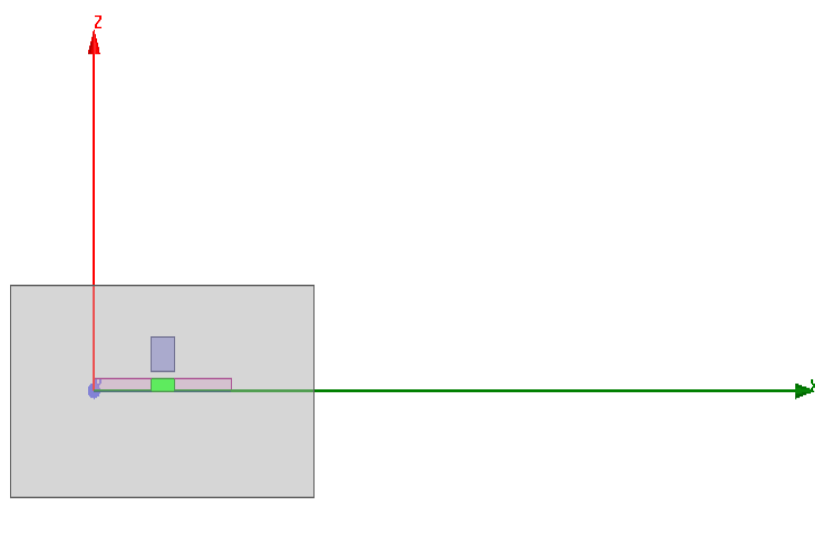


Figure 3.7: Simulation setup for MUT at a height 1mm above sensor

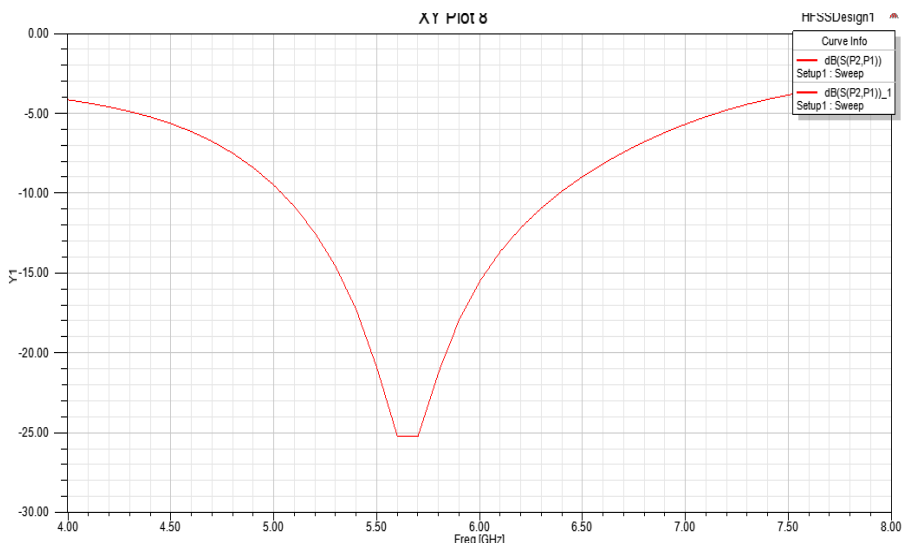


Figure 3.8: S21 for MUT at a height 1mm above sensor

Here a flattening in S21 occurs because the frequency sweep has to be increased, which could increase the simulation time.

3.4.3 CASE 3

MUT was kept above the sensor in contact with it. The corresponding simulation part in HFSS and the S21 characteristics obtained are given in Fig 3.9 and Fig 3.10. This is considered to be the ideal position for MUT.

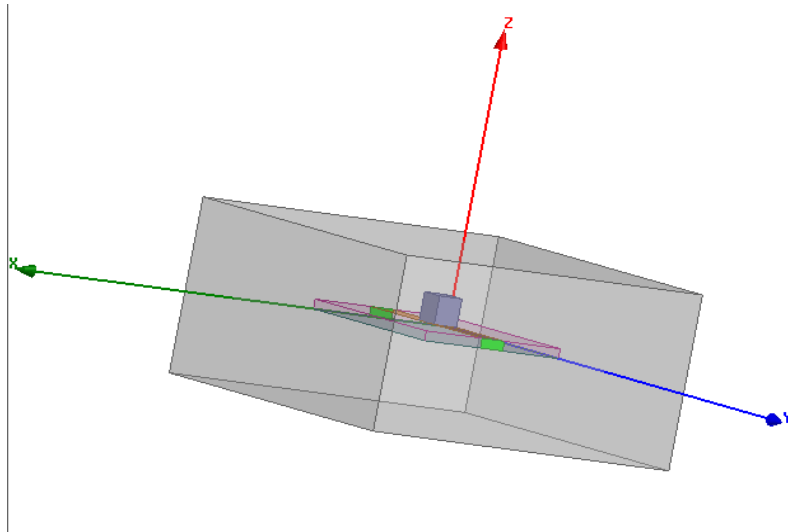


Figure 3.9: Simulation setup for MUT in contact with the sensor

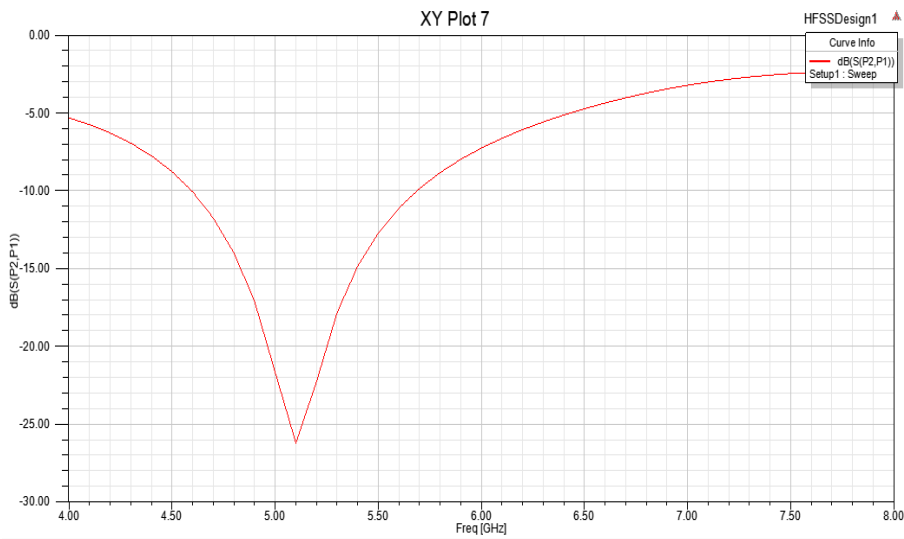


Figure 3.10: S21 for MUT in contact with the sensor

3.4.4 CASE 4

Varying the materials for the MUT observe the corresponding S21 characteristic for different materials starting from air having relative

permittivity (1.008) to fresh water having permittivity (81). Some of the simulation results are given in Fig 3.11, 3.12, 3.13 and 3.14.

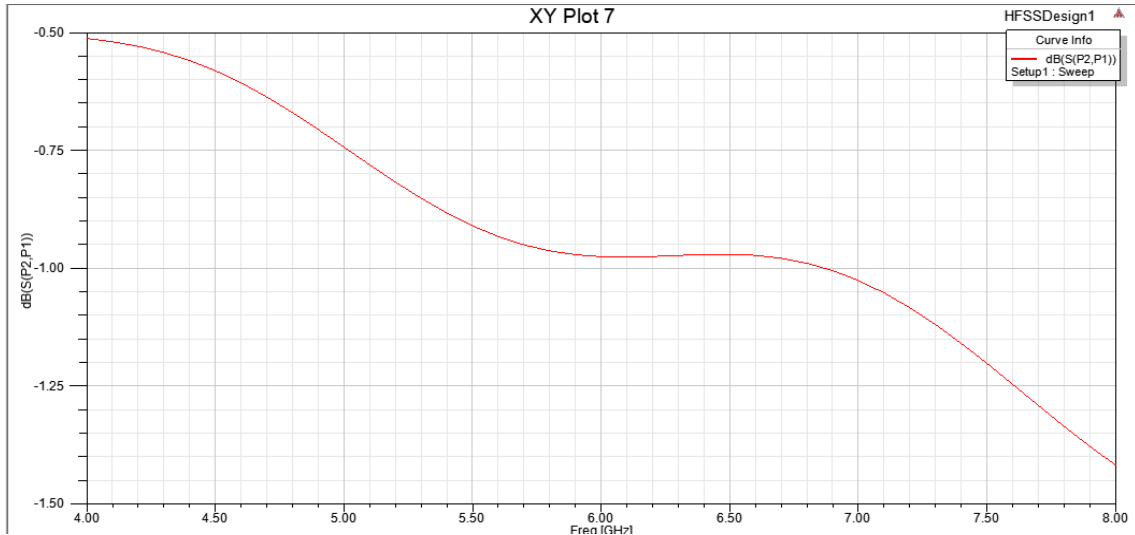


Figure 3.11: S21 of air with relative permittivity=1.008

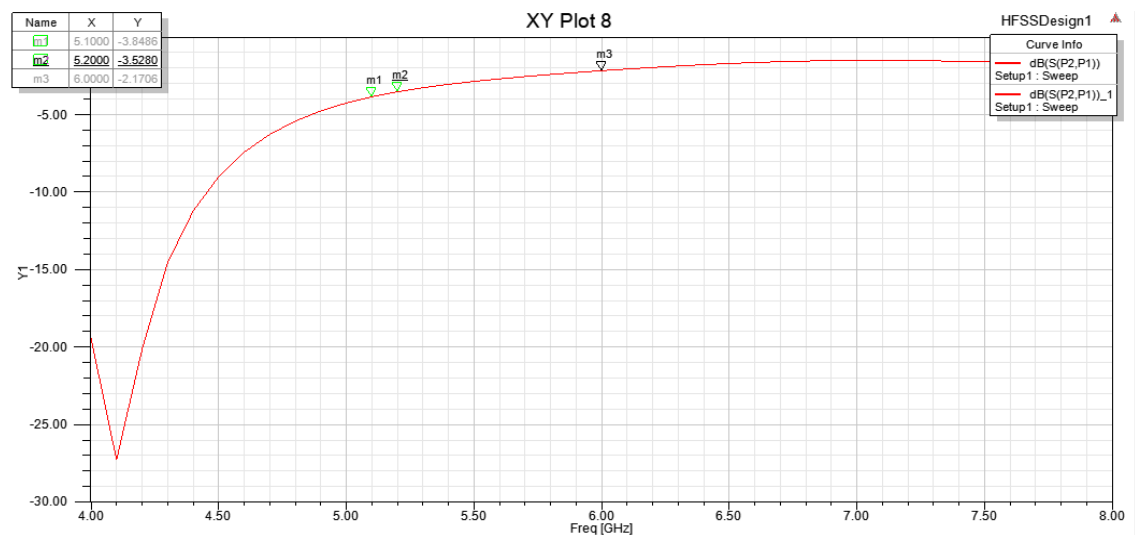


Figure 3.12: S21 of material with relative permittivity=5.7

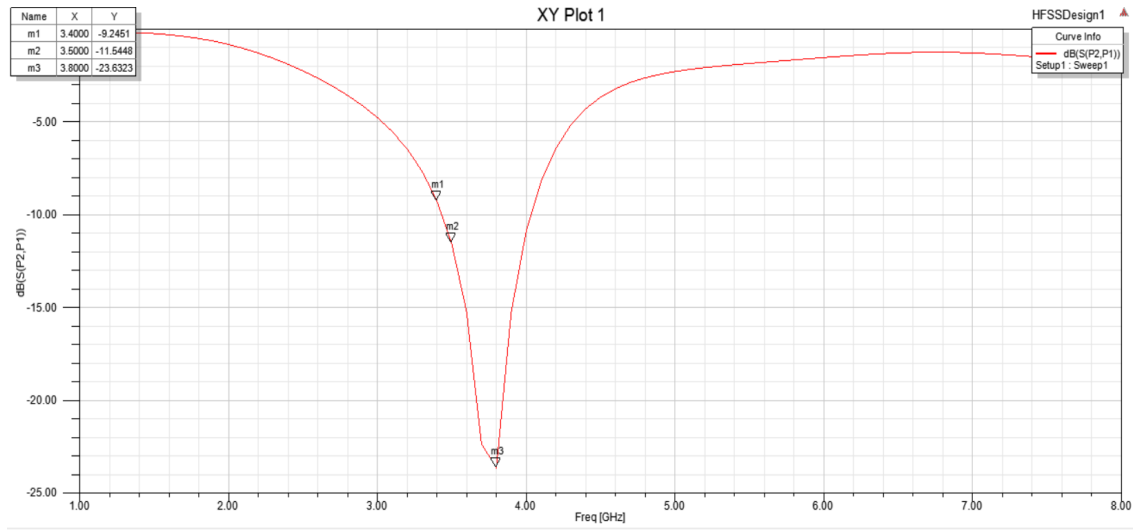


Figure 3.13: S21 of material with relative permittivity=6.8

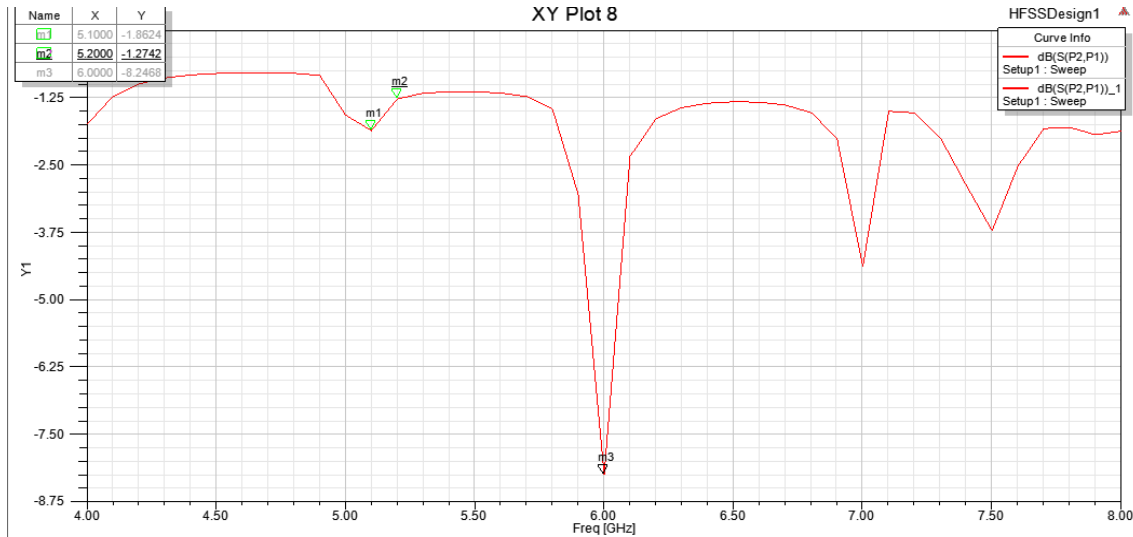


Figure 3.14: S21 of fresh water with relative permittivity=81

3.4.5 CASE 5: VOLUMETRIC ANALYSIS

The next major thing which affected the shift was volume of the MUT, so to choose an different volumes for MUT were tested. The volumes for which simulations performed are 8 cubic.mm, 27 cubic.mm, 75.2 cubic.mm and 125 cubic.mm. The corresponding resonant frequency obtained for each volume by varying permittivity is shown in the table 1. For better analytical perspective graphical representation is more. The graphical representation of table 1 is shown in figure 3.15. From this we can derive a

conclusion that above 75.2 cubic.mm volume there is no considerable effect of volume in resonant frequency so the minimum volume of MUT kept for correct results should be more than 75.2 cubic.mm. From the data obtained the final position of MUT is above the IDC structure and the volume of the MUT should not be less than 75.2 cubic.mm. The volume of MUT for modeling is arbitrarily chosen as 88.36 cubic.mm.

Table 3.1: Volumetric analysis table

Volume(mm^3) \ Permittivity	2.33	2.44	2.6	3.87	6.15	6.5	13.8
$2 \times 2 \times 2$	5.4889	5.4688	5.4447	5.339	5.1396	5.1183	4.5382
$3 \times 3 \times 3$	5.3357	5.3213	5.2883	5.0581	4.7116	4.6633	4.0011
$4 \times 4.7 \times 4$	5.0068	4.9619	4.9026	4.521	4.0032	3.9537	2.8525
$5 \times 5 \times 5$	4.98	4.9484	4.8742	4.4338	3.8829	3.8288	2.1803

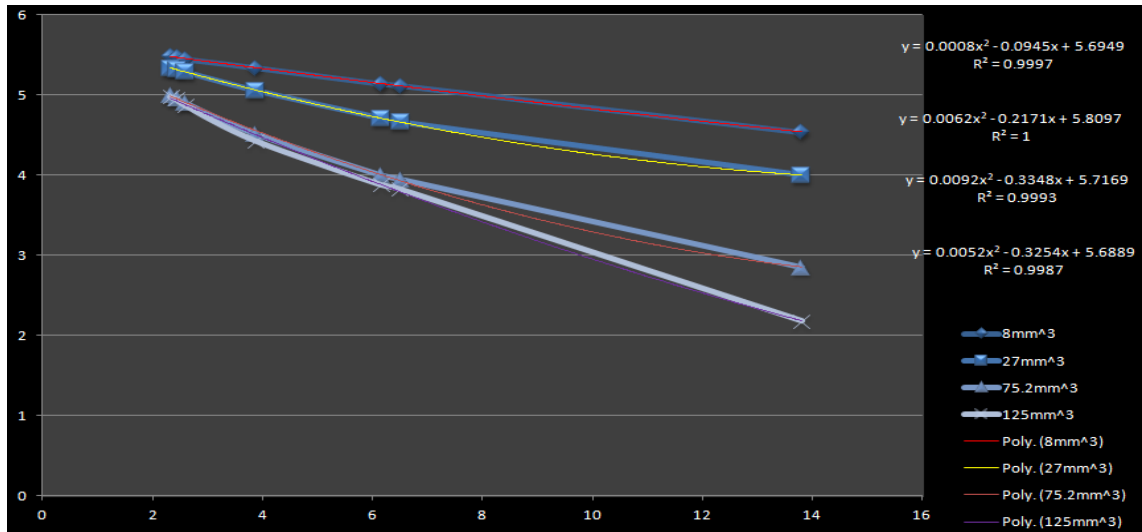


Figure 3.15: Volumetric Analysis

3.5 MODELLING

After simulation of materials with different permittivity the data obtained is converted to a numerical model, relative permittivity and corresponding resonant frequency obtained for various materials are shown in table 2. From the data obtained the parameters are plotted in a graph to give a better analytical view. Permittivity values are plotted along x-axis and

corresponding resonant frequency obtained for each material is plotted along y-axis. A graph which represents the inverse proportional relation is obtained; the figure 3.16 shows this relation.

Table 3.2: Resonant Frequency Vs Relative Permittivity

Materials	Relative Permittivity	Resonant frequency
Air	1.0006	5.7
Polyflon Cuflon	2.1	5
Neltec NY9220(IM)	2.2	5
Oil	2.33	5.01
Loamy Soil dry	2.44	4.96
Neltec NX9245(IM)	2.45	4.9
Sandy soil dry	2.53	4.92
Preperm L255	2.55	4.92
Preperm L260	2.6	4.9
Preperm L270	2.7	4.87
Taconic TLC	2.75	4.86
Arlon CLTE-XT	2.94	4.9
Preperm L300	3	4.78
Preperm L330	3.3	4.68
Krempel Akaflex KCL	3.4	4.6
Paper oil impregnated	3.87	4.52
BT systems	3.9	4.6
Arlon AD450	4.5	4.4
diamond hi pres	5.7	4.1
Arlon AD 600	6.15	4.01
Beryllia	6.5	3.95
Be O	6.8	3.7
Al N	8.8	3.5
alumina 96pct	9.4	3.4
Al ₂ O ₃ ceramic	9.8	3.35
Arlon AR1000	10	3.3
Arlon AD1000	10.2	3.3
Silicon	11.9	3.1
GaAs	12.9	3
Sandy soil wet	13	2.81
Loamy Soil wet	13.8	2.85
Diamond	16.5	2.8
Glycerin	50	1.79
Water liquid 20C	78	1.28
Fresh water/Distilled water	81	1.4

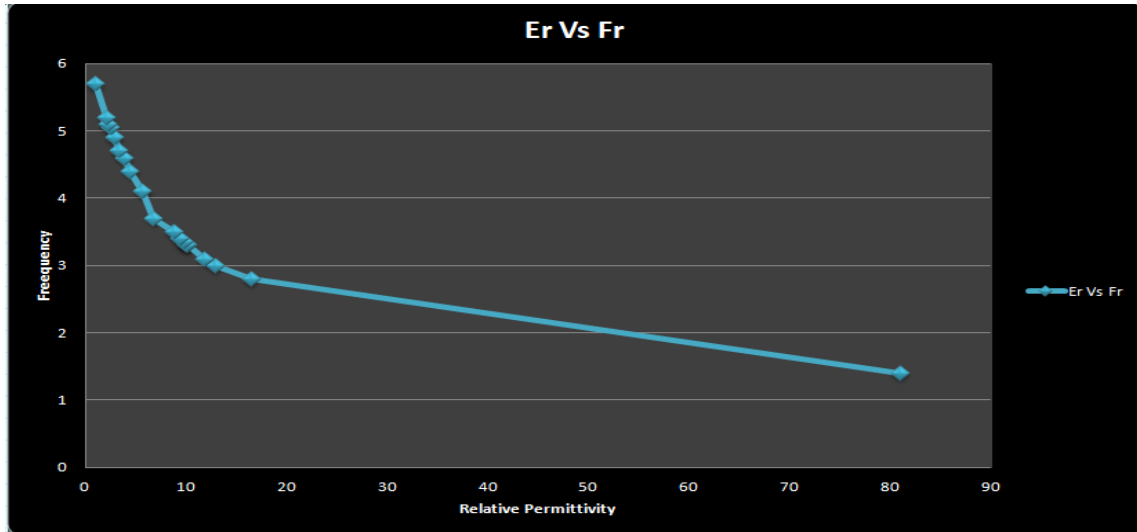


Figure 3.16: Relative permittivity v/s Resonant frequency

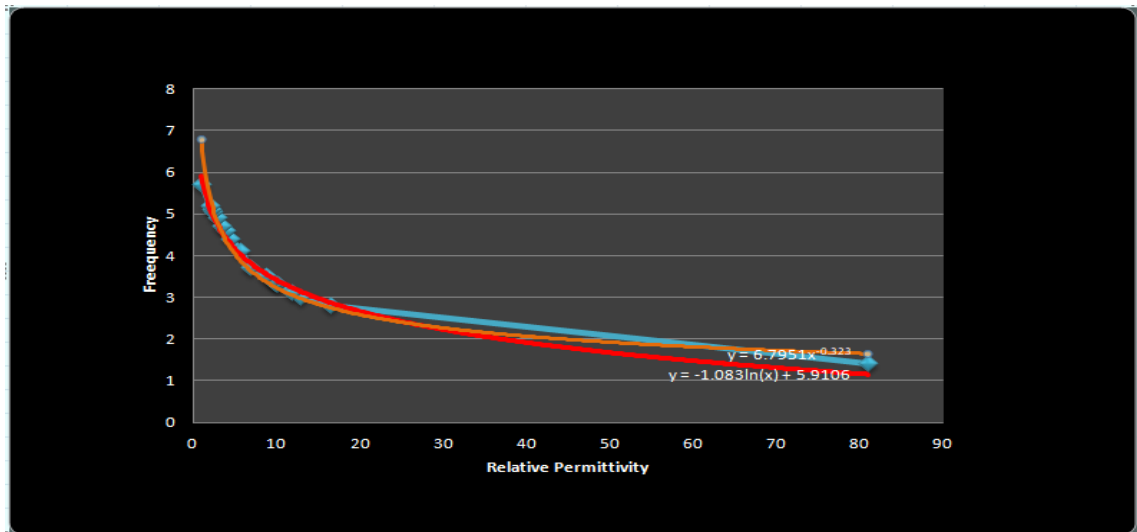


Figure 3.17: Approximation of the dataset using logarithmic and power functions

Graph shown in figure 3.16 has to be approximated to obtain suitable model, for this regression analysis over this was performed, power and logarithmic function were the two functions which gave the best results as shown in figure 10. Among these two functions logarithmic function was more accurate and it corresponds to the model as shown in figure 3.17. The corresponding equation of the model is given below,

$$Fr = -1.083 \times \ln(\epsilon_r) + 5.9106 \quad (3.1)$$

Chapter 4

Fabrication and Testing

4.1 Fabrication of Sensor antenna

The data set was acquired and corresponding model is created after that antenna is fabricated. There are various methods for antenna fabrication; firstly milling method for removal of copper to obtain feed line was employed. It was noticed that due to excessive milling the required structure was not accurately obtained. The next technique used for fabrication is photolithography. This is a chemical etching process by which the unwanted metal regions of the metallic layer are removed so that the intended design is obtained. Depending upon the design of the antenna as biplanar or uniplanar dual or single side substrates are used. The selection of a proper substrate material is the essential part in antenna design process.

The selection of dielectric constant of the substrate depends on the application of the antenna and the radiation characteristics specifications. High Dielectric constant substrates causes' surface wave excitation and low bandwidth performance. Also as the frequency of operation increases, the loss tangent of the material used for substrates slightly increases, which in turn adversely affects the efficiency of the antenna. Also increasing the thickness of the substrate increases the band width of the antennas at the expense of efficiency owing to increase in surface waves. FR4 with $\epsilon_r=4.4$,

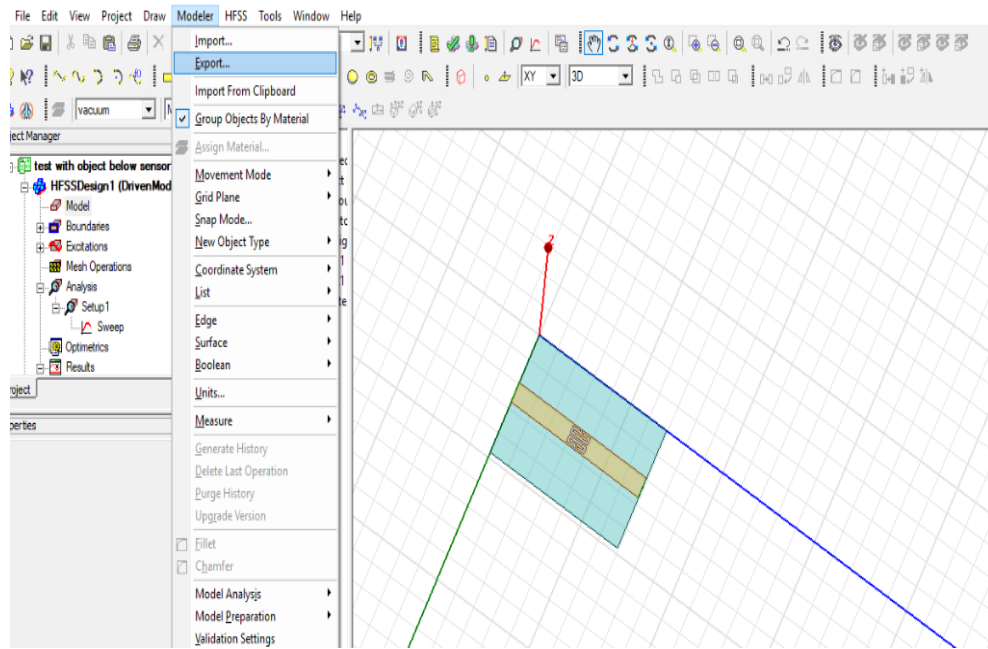


Figure 4.1: Placing structure in x-y plane

$\tan\delta=.02$, $h=1.6$ mm is used for this implementation[24].

4.1.1 Photolithography

After the proper selection of the substrate material a computer aided design of the geometry is initially made and a negative mask of the geometry to be generated is printed on a transparent sheet. The simulation was done on 3D structure in ANSYS HFSS; from the HFSS software the structure was exported into .dxf format drawing exchange format. The portion of the structure which has to converted to mask should be kept in the x-y plane before converting. The conversion of structure to .dxf format is shown in figures 4.1 and 4.2. Using this file mask should be created for this Coreldraw can be used, the .dxf file is imported to Coreldraw and the required changes are made and a negative mask is created. The copper part of the feed is shown in black and all the other portions are kept white in color as shown in figure 4.3.

A double sided substrate with copper metallization of suitable dimension is



Figure 4.2: Saving the file

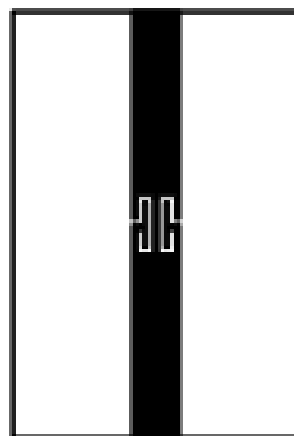


Figure 4.3: Structure printed in transparent sheet

properly cleaned using acetone to free from impurities. A thin layer of negative photo resist solution (1:1 mix of negative photo resist solution and thinner) is coated using spinning technique on copper surfaces and is dried. The mask is placed onto the photo resist and exposed to UV light. After the proper UV exposure the layer of photo-resist material in the exposed portions hardens when it is treated with developer solution. The board is then dipped in dye ink solution in order to clearly view the hardened photo resist portions on the copper coating; the board is then washed in water. After developing phase the unwanted copper portions are etched off using Ferric Chloride (FeCl_3) solution to get the required antenna geometry on the substrate. The etched board is rinsed in running water to remove any etchant. FeCl_3 dissolves the copper parts except underneath the hardened photo resist layer after few minutes. The laminate is then cleaned carefully to remove the hardened photo resist using acetone solution.

After the fabrication process the required antenna structure should be removed from the parent structure, for this laser cutting was used but it gave poor result. To obtain a better structure and machine cutting was used, it provided clean structure. After all these steps the antenna is fabricated as per requirement as shown in figure 4.4.

4.2 Experimental Setup

This section explains about the techniques of experiment with antenna, an epigrammatic overview of the equipments and facilities used for extracting the antenna reflection and radiation characteristics is presented in this section. The measurement of radiation characteristics of the antennas were carried out using Network analyzer VNA Master 2026C by Anritsu.



Figure 4.4: Fabricated antenna

4.2.1 VNA Master 2026C

The VNA Master MS202xC/3xC series is made up of the industry's highest performance, fully reversing handheld vector network analyzers (VNA) with frequency coverage from practically DC (5 kHz) to 6, 15 or 20 GHz. With an available high-performance spectrum analyzer covering 9 kHz to 9, 15 or 20 GHz, the VNA Master series transforms into a powerful multi-function instrument capable of enabling field technicians and engineers to accurately install, troubleshoot and maintain complex communication systems with the highest degree of accuracy and reliability. Whether it's a mission critical military application or simply a consumer services type of application, the VNA Master series will provide accurate and dependable measurements anytime, anywhere. The VNA Master has a 2-port, 2-path architecture that automatically measures four S-parameters with a single connection. There are three receivers, so the forward sweep from Port 1 simultaneously yields S₁₁ and S₂₁, and the reverse sweep from Port 2 simultaneously yields S₂₂ and S₁₂. The four S-parameters for a two-port device under test require only two sweeps, both forward and reverse transmission. With just one



Figure 4.5: VNA Master 2026C front view

connection, the VNA Master provides both precision measurements and hands-free operation[25]. The VNA used is shown in figure 4.5 and 4.6.

The material under test (MUT) is connected to the port of the S-parameter test set VNA Master 2026C and the forward and reflected power at the measurement point is separated and down converted to 20MHz using frequency down converter. It is again down converted to lower frequency and processed in the processing unit. All the systems discussed above are interconnected using VNA Master 2026 bus. A computer interfaced to the system is used for coordinating the whole operation remotely. Measurement data can be saved on a storage medium.

4.3 Antenna Testing

The antenna sensor for testing needed to be connected with VNA, the connector used should be as per requirements of VNA. N type connectors were used to connect sensor antenna as shown in figure 4.7.



Figure 4.6: VNA Master 2026C back view

The experimental procedures followed to determine the antenna characteristics are, power is fed to the antenna from the S parameter test set of the analyzer through cables and connectors. The connectors and cables tend to be lossy at higher microwave bands. Hence the instrument should be calibrated with known standards of open, short and matched loads to get accurate scattering parameters. There are many calibration procedures available in the network analyzer. Single port and full two port calibration methods are usually used. Return loss, VSWR and input impedance can be characterized using single port calibration method.

The fabricated antenna is tested by measuring the S₂₁ scattering parameter and the antenna tested alone provided result that matched the simulation result.



Figure 4.7: Final structure

Chapter 5

Conclusion

This project gives an overview of the microwave sensor technologies for food properties measurement, identifies the limitations of the conventional technologies in food quality measurement and proposes the potential solutions. In summary, the lessons learned are:

1. Study microwave sensors and microwave characteristics of food.
2. Microwave sensor is sensitive to food quality variation and the wide range frequency is promising to obtain different features and microwave dielectric measurement is a suitable method for food evaluation due to its nature of contact-less, hygienic and non-destructive.
3. Real time analysis of adulterants in food item can be predicted from the data obtained from VNA using algorithm.
4. The proposed sensor is working at the industrial, scientific and medical (ISM) band frequency of 5.7 GHz.
5. Since the sensor model can be scaled to any other frequency band, the overall design can also be made applicable for characterization of food adulteration at other designated ISM frequency bands.

Bibliography

- [1] Nondestructive Technique for Detection of Adulteration in Edible Oils using Planar RF Sensor Muhammed Shafi K T, Abhishek Kumar Jha, and M Jaleel Akhtar Department of Electrical Engineering, Indian Institute of Technology Kanpur, India
- [2] Meng Z, Wu Z, Gray J (2017); Microwave Sensor Technologies for Food Evaluation and Analysis – Methods, Challenges and Solutions. Transactions of the Institute of Measurement and Control. <https://doi.org/10.1177/0142331217721968>
- [3] Posudin, Yuriv Peiris, Kamaranga Kays, Stanley. (2015). Non-destructive Detection of Food Adulteration to Guarantee Human Health and Safety.. Ukrainian Food Journal. 4. 207 - 260.
- [4] Terracini B. (2004), Toxic oil syndrome. Ten years of progress, World Health Organization Regional Office, Copenhagen.
- [5] Roth V., Tsay A.A., Pullman M.E., Gray J.V. (2008), Unraveling the food supply chain: strategic insights from China and the 2007 recalls, J. Supply Chain Management, 44, pp. 22-44.
- [6] Kolb B., Ettre L.S. (2006), Static headspace-gas chromatography: Theory and practice, 2nd edition, Wiley-Interscience, New York (NY).
- [7] Hai Z., Wang J. (2006), Electronic nose and data analysis for detection of maize oil adulteration in sesame oil., Sensors and Actuators B: Chemical, 119(2), pp. 449-55.

- [8] Compton D.A., Compton S.V. (1991), Examination of packaged consumer goods by using FT-Raman spectrometry, *Applied Spectroscopy*, 45(10), pp. 1587-9.
- [9] Zhang X.F., Zou M.Q., Qi X.H., Liu F., Zhu X.H., Zhao B.H. (2010), Detection of melamine in liquid milk using surface-enhanced Raman scattering spectroscopy, *J. Raman Spectroscopy*, 41(12), pp. 1655-60.
- [10] Alampresea C., Casaleb M., Sinellia N., Lanterib S., Casiraghia E. (2013), Detection of minced beef adulteration with turkey meat by UV-vis, NIR and MIR spectroscopy, *Food Sci. Technol.*, 53(1), pp. 225–232.
- [11] Rohman A., Erwanto Y., Che Man Y.B. (2011), Analysis of pork adulteration in beef meatball using Fourier transform infrared (FTIR) spectroscopy, *Meat Sci.*, 88, pp. 91-5.
- [12] Ding H.B., Xu R.J. (2000), Near-infrared spectroscopic technique for detection of beef hamburger adulteration, *J. Agric. Food Chem.*, 48(6), pp. 2193-8.
- [13] Jaiswal P.K. (2010), High-performance thin-layer chromatography in food analysis, CBS Pub., New Delhi, India.
- [14] Hilali M., Charrouf Z., El Aziz Soulhi A., Hachimi L., Guillaume D. (2007), Detection of argan oil adulteration using quantitative campesterol GC-analysis, *J. Amer Oil Chem Soc.*, 84, pp. 761-4.
- [15] Opara U.L., Pathare P.B. (2014), Bruise damage measurement and analysis of fresh horticultural produce – A review, *Postharvest Biol. Technol.*, 91, pp. 9-24.
- [16] Lee W.H., Kim M.S., Lee H., Delwiche S.R., Bae H., Kim D.Y., Cho B.K. (2014), Hyperspectral near-infrared imaging for the detection of physical damages of pear, *J. Food Engineering*, 130, pp. 1-7.

[17] Vigli G., Philippidis A., Spyros C., Dais P. (2003), Classification of edible oils by employing ^{31}P and ^1H NMR spectroscopy in combination with multivariate statistical analysis. A proposal for the detection of seed oil adulteration in virgin olive oils, *J. Agric. Food Chem.* 51, pp. 5715-22.

[18] Ferrari E., Foca G., Vignali M., Tassi L., Ulrici A. (2011), Adulteration of the anthocyanin content of red wines: Perspectives for authentication by Fourier transform-near infrared and ^1H NMR spectroscopies, *Analytica Chimica Acta*, 701(2), pp. 139-51.

9

[19] Mannaş D, Altuğ T. (2007), SPME/GC/MS and sensory flavour profile analysis for estimation of authenticity of thyme honey., *Intern. J. Food Sci. Technol.*, 2(2), pp.133-8.

[20] Reid L.M, O'Donnell C.P, Downey G. (2004), Potential of SPME-GC and chemometrics to detect adulteration of soft fruit purées., *J. Agric. Food Chem.*, 52, pp. 421-7.

[21] Bojanic, R., Milosevic, v., Jokanovic, B., Medina-Mena, F. and Mesa, F., "Enhanced modelling of split-ring resonators couplings in printed circuits," *IEEE Trans. Microw. Theory Tech.*, vol. 62, no. 8, pp. 1605-1615, Aug. 2014.

[22] Jha, A K. and Akhtar M. 1., "Automated RF measurement system for detecting adulteration in edible fluids," *Applied Electromagnetics Conference (AEMC)*. Bhubaneswar, 2013, pp. 1-2.

[23] N. Dib and L. Katehi, "Modeling of shielded CPW discontinuities using the space domain integral equation method (SDIE)," *J. Electromagnetic Waves Applicat.*, vol. 5, pp. 503–523, Apr. 1991.

[24] M. T. Sebastian, "Dielectric materials for wireless communications," Elsevier publishers UK., (2008).

[25] <https://www.anritsu.com/en-US/test-measurement/support>